THE PLANETARY-SCALE CIRCULATION OF THE UPPER TROPICAL TROPOSPHERE AND ITS INFLUENCE ON TROPICAL WEATHER

A Dissertation
Presented to
The Academic Faculty

by

Sebastián Ortega Arango

In Partial Fulfillment
of the Requirements for the Degree
Doctor of Philosophy in the
School of Earth and Atmospheric Sciences

Georgia Institute of Technology
December 2016

THE PLANETARY-SCALE CIRCULATION OF THE UPPER TROPICAL TROPOSPHERE AND ITS INFLUENCE ON TROPICAL WEATHER

Approved by:

Dr. Peter J. Webster, Advisor
School of Earth and Atmospheric Sciences
Georgia Institute of Technology

Dr. Predrag Cvitanović
School of Physics
Georgia Institute of Technology

Dr. Judith A. Curry
School of Earth and Atmospheric Sciences
Georgia Institute of Technology

Dr. Yi Deng
School of Earth and Atmospheric Sciences
Georgia Institute of Technology

Dr. Annalisa Bracco
School of Earth and Atmospheric Sciences
Georgia Institute of Technology

Date Approved: October 04, 2016

To Josefina, this is also her achievement

ACKNOWLEDGEMENTS

This work would have never been possible without the constant love, support, and encouragement of both family and friends. I am deeply grateful to all of them. I thank my PhD advisor and mentor, Dr. Peter J. Webster, for his invaluable guidance and support throughout my graduate studies. His insatiable scientific curiosity, and his openness to new ideas, made this work much better than it would had otherwise been. I thank the current and former members of Dr. Webster's group and the students, faculty, and staff of the School of Earth and Atmospheric Sciences at GeorgiaTech. I am grateful for having been a part of such encouraging, stimulating, and friendly environment. I extend my gratitude to all the members of my doctoral committee. Their guidance, as well as the important lessons that I learned while taking their classes, will always prove invaluable.

TABLE OF CONTENTS

LIST OF FIGURES

LIST OF SYMBOLS AND ABBREVIATIONS

PV, q	Potential vorticity
UQBW	Upper tropospheric quasi-biweekly oscillation
QBW	Lower tropospheric quasi-biweekly oscillation
OLR	Outgoing long-wave radiation
VIMT	Volume-integrated horizontal moisture transport
EEOF	Extended Empirical Orthogonal Function
MPV	Maximum potential vorticity (over peninsular India)
ERA-Interim	A reanalysis from the European Centre for Medium-Range Weather Forecasts
NOAA	National Oceanic and Atmospheric Administration
$\boldsymbol{v}$	Velocity vector
u	Zonal velocity component
$\boldsymbol{\omega}$	Absolute vorticity vector
$\boldsymbol{k}$	Vertical unit vector
$\boldsymbol{n}$	Vector that points towards the equator along a latitude circle
η	Vertical component of the absolute vorticity
ξ	Vertical component of the relative vorticity
f	Coriolis parameter
ρ	Density
σ	Mass density on isentropic coordinates
$\boldsymbol{J}$	PV flux
$\boldsymbol{J_A}$	Advective PV flux
$\boldsymbol{J_{\dot{\theta}}}$	Diabatic PV flux

$\boldsymbol{J_F}$	Frictional PV flux
$\boldsymbol{F}$	Frictional processes vector
h	Height of the shallow water model
h_e	Relaxation height of the shallow water model
τ	Relaxation height timescale
H	Reference height of the shallow water model
g	Gravitational constant
θ	Potential temperature
S	Mass sources and sinks
A	Amplitude of the mass forcing
λ	Longitude
ϕ	Latitude
N	Brunt–Väisälä frequency
K_E	Kinetic energy
M	Montgomery stream function
k	Linear dissipation coefficient
R	Earth's radius

SUMMARY

Through observational analyses, we suggest that the upper tropospheric potential vorticity (PV) field has an effect on the lower troposphere during the South Asian monsoon. We show that the variability of the upper tropospheric PV field during the monsoon has a strong quasi-biweekly component, and characterize the evolution of the PV field as Rossby waves that travel eastward on the subtropical jets, that break over the Pacific Ocean, and that are advected westward on the equatorial westerly winds as eddies and PV streamers that are remnants of these breaking Rossby waves. We then show that this upper tropospheric variability coevolves with the lower tropospheric quasi-biweekly oscillations of the South Asian Monsoon.

Through an analytical argument, we provide an explanation for the existence of the upper tropospheric variability. First, we show that the breaking Rossby waves generate equatorward fluxes of PV throughout the year, and that these fluxes are closely compensated by poleward fluxes of PV that are generated by deep tropical convection. Using the impermeability theorem of the atmosphere, we show that these advective fluxes must always occur and, if advective processes are of first order importance, they should be expected to closely balance. Moreover, we suggest that imbalances in these advective fluxes help maintain the circulation of the upper troposphere, and show how this is exactly the case for a shallow water model of the atmosphere. We comment on the implications that this work has for our understanding of the tropical atmosphere.

CHAPTER 1. INTRODUCTION

In a paper of historical significance, Hadley (1735) put forward a view of the tropical atmospheric circulation that persists, with some modifications, until today. Hadley perceived a zonally symmetric atmosphere, one that does not vary with longitude, and sought the implications of heating the atmosphere around the tropics.

Hadley first suggested that a meridional circulation would develop. He reasoned that warmer temperatures over the tropics would cause air parcels to become buoyant[1] and rise to the upper troposphere, generating a low-pressure belt in the lower troposphere and a high-pressure belt in the upper troposphere. Thus, air parcels in the lower troposphere would converge towards the tropics and air parcels in the upper troposphere would diverge towards the poles. The upper tropospheric parcels would also slowly sink back to the lower troposphere as they cooled, and would eventually reach the lower troposphere over midlatitudes.

Hadley then suggested that such meridional circulation would lead to the creation of the prevailing lower tropospheric winds. He assumed that moving air parcels would tend to conserve some of their zonal velocity, while losing some to frictional effects. And then reasoned that, if the atmosphere where to be initially at rest, air parcels over midlatitudes would have a smaller zonal velocity than those over the equator. Thus, air parcels

[1] Hadley actually uses the term "rarified" instead of "buoyant", as well as using many other terms that are not standard in today's meteorological vocabulary. Yet, all can be easily translated or corrected.

converging towards the equator would seem to gain an easterly component and those diverging toward the poles would seem to gain a westerly one. This, he suggested, would lead to the creation of the lower tropospheric trade winds over the equator and the westerly winds over midlatitudes.

We now know that Hadley was wrong in several steps of his reasoning (Lorenz 1967). He was wrong in assuming that air parcels would tend to conserve their absolute velocity, while in reality air parcels tend to conserve their angular momentum. He was wrong in assuming that the upper branch of the circulation would explain the prevailing lower tropospheric westerlies at midlatitudes, while in reality midlatitude cyclones are responsible for these prevailing winds. And, among other flaws, he was wrong in neglecting the importance that deep convective clouds would have in the meridional circulation. Yet, his reasoning led him to the right qualitative result for the tropical atmosphere: a meridional circulation with easterlies over the equator and westerlies in the upper troposphere.

Hadley's paper was followed[2] by attempts to fit his zonally symmetric view to new observations of the global circulation (Lorenz 1967; Lorenz 1983). However, around the 1900's it was recognized that the assumption of zonal symmetry was particularly strong for the midlatitudes (Lewis 1998). The weather of the midlatitudes, as well as its meridional circulation and its prevailing winds, was shown to be dominated by midlatitude cyclones. A zonally symmetric circulation could not represent these cyclones, and Hadley's view was disregarded as the plausible explanation of the global atmospheric circulation.

Modern studies have looked back at Hadley's ideas as being relevant at least for the tropical atmosphere. Schneider and Lindzen (1977) coded the equations of mass, momentum, and energy for a zonally symmetric model of the atmosphere, and showed that a tropical circulation similar to that described by Hadley could develop. Held and Hou (1980) gave quantitative predictions of various aspects of a zonally symmetric tropical circulation by using simple axioms similar to those of Hadley; for instance, one of such axioms was assuming that the upper branch of the circulation conserves its angular momentum. They predicted that the latitudinal extent of the meridional circulation would be about 30°N and

[2] The studies here referred are those of Ferrel and Thomson. Yet, these studies were published over a century after Hadley had published his ideas. Hadley's ideas were widely ignored after their publication. The incorrect ideas of Halley (instead of Hadley), that the winds followed the sun's motion, were the accepted status quo at the time, and had inertia of their own. Hadley's ideas were slowly rediscover by several individuals, including Kant, Laplace, De Luc, Dove, and Dalton, the last two responsible for crediting them back to Hadley (Persson 2006).

30°S, that the subtropical westerly jets would develop in the upper troposphere where Hadley's cell ends, and that the distribution of surface winds would have easterlies over the equator and westerlies elsewhere. Further, they corroborated their predictions with a zonally symmetric model.

Moreover, the studies of Lindzen and Hou (1988) and Plumb and Hou (1992) built on the work of Held and Hou, and suggested explanations for the observed north-south asymmetries in the meridional circulation of the tropical atmosphere. Lindzen and Hou showed that a strongly asymmetric circulation developed in their zonally symmetric model when deep convection[3] was located just a few degrees away from the equator. And Plumb and Hou showed that a strong cross equatorial circulation would develop in their zonally symmetric model when deep convection was located over the midlatitudes and the amplitude of the convective forcing was set to be sufficiently large so that the absolute

[3] A note of caution is needed here. Deep convection should not be thought of as an external forcing of the circulation. Rather, it should be thought as a response of the atmosphere to a meridional temperature gradient that is set up by the radiative process in the Sun-Earth system. That is, as discussed in Emanuel et al. (1994), diabatic heating is not the driver of the circulation, but a part of it that greatly modifies it. Nonetheless, studies that make the assumption that deep convection forces the circulation are still of interest. They show the large-scale dynamical response of the atmosphere given the distribution of deep convection, separating the large-scale dynamics from the convective dynamics, and giving insight into how they might interact.

vorticity of the upper troposphere would vanish. Thus, also suggesting an explanation for the abrupt onset of the monsoon.

Yet, by the time the papers of Held, Lindzen, Plumb, and Hou were published, it was already clear that zonally asymmetric quasi-geostrophic motions were also important in shaping the circulation of the tropical atmosphere. Matsuno (1966) famously showed that a perturbation in a tropical atmosphere would translate into equatorially trapped planetary waves for which quasi-geostrophic motions were important: inertia-gravity waves, Rossby, and Kelvin waves would develop as a response to such perturbation. Moreover, Webster (1972) and Gill (1980) showed that such waves would play an important role in shaping the observed circulation of the tropical atmosphere, leading to a decisively zonally asymmetric pattern, characteristic of the upper and lower tropical troposphere.

Theoretical studies of the tropical upper troposphere reinforced the importance of the zonal asymmetries. The studies of Webster (1973), Webster and Holton (1982), and Webster and Chang (1998), showed that a zonally asymmetric basic flow in the upper troposphere would lead to the propagation of extratropical Rossby waves into the tropics through equatorial regions of westerly winds, termed “westerly ducts”. The observational studies that followed confirmed the propagation of such Rossby waves into the tropics and detailed their characteristics (Kiladis and Weickmann 1992; Tomas and Webster 1994). Moreover, such observational studies showed that tropical convection was usually observed in association with the transit of these waves through the westerly ducts, partially supporting previous suggestions of Charney (1963) that extratropical atmosphere should have a direct influence on tropical weather.

The way in which these extratropical Rossby waves propagated into the tropics was further clarified by studies that considered the potential vorticity (PV) field[4] of the upper troposphere (Postel and Hitchman 1999; Slingo 1998; Waugh and Polvani 2000). By focusing on the PV field, these studies revealed the nonlinear behavior of the tropical upper troposphere, with troughs and ridges of the PV field, associated with Rossby waves, breaking[5] and mixing when propagating over the westerly ducts (Scott and Cammas 2002; Scott et al. 2001). Moreover, insights into how they affect the lower troposphere and initiate tropical convection was also achieved considering the PV of these waves (Funatsu and Waugh 2008; Knippertz 2007; Masarik and Schubert 2013).

In this work we attempt to further advance the understanding of the effect that Rossby waves have on the tropical upper and lower troposphere. In Chapter 2, we give insight into how the variability of the upper troposphere might affect the lower troposphere during the monsoon. We show that the quasi-biweekly oscillation of the upper troposphere (Hsu and Plumb 2000; Liu et al. 2007; Popovic and Plumb 2001) coevolves with the quasi-biweekly oscillations of the lower troposphere (Annamalai and Slingo 2001; Kikuchi and Wang 2009) and discuss how this might be important for the formation of tropical cyclones (Ortega et al., 2016a).

[4] The PV field will be discussed extensively in Appendix A. For now, it suffices to know that the PV field is related with the absolute vorticity and vertical stability of the flow, that it tends to be conserved, and that its perturbations lead to the formation of Rossby waves.

[5] The definition of Rossby wave breaking will also be discussed in Appendix A.

In Chapter 3, we provide insight into why this upper tropospheric variability should always be expected. We show that the tropics and extratropics are intrinsically linked via Rossby-wave dynamics and that not only do the extratropics affect weather in the tropics, as Charney (1963) would suggest, but that the tropics also have a clear effect on the extratropics via deep convection and the divergent circulation it generates, as discussed by Slingo (1998) and Ortega et al. (2016b).

Chapters 2 and 3 constitute the core of this thesis and assume a basic knowledge of atmospheric dynamics. In particular, they assume basic knowledge of the ideas behind PV. Thus, it is convenient to review these concepts as a foundation for the chapters to follow. A brief review can be found in Appendix A at the end of this thesis. More detailed information can be found in the review papers of Hoskins et al. (1985), McIntyre (2001), McIntyre (2003b), and Hoskins (2015).

CHAPTER 2. QUASI-BIWEEKLY OSCILLATIONS OF THE SOUTH ASIAN MONSOON AND ITS CO-EVOLUTION IN THE UPPER AND LOWER TROPOSPHERE

Sebastián Ortega, Peter J. Webster, Violeta Toma, Hai-Ru Chang
This work is currently under a second round of revisions, and under consideration for publication, in the journal Climate Dynamics.

2.1 Introduction

The South Asian Monsoon displays strong intraseasonal variability on 10-20 and 30-60 day timescales (e.g., Krishnamurti and Ardanuy 1980; Annamalai and Slingo 2001; Lawrence and Webster 2002; Hoyos and Webster 2007; Kikuchi and Wang 2009; Lee et al. 2012). Over central India, rainfall varies prominently on these timescales, leading to "active" and "break" periods for which the rainfall is, respectively, well above and below the climatological mean (Sikka and Gadgil 1980; Webster et al. 1998; Webster and Hoyos 2004; Hoyos and Webster 2007; Goswami 2012).

The variability on 30-60 day timescales, referred to as the Monsoon Intraseasonal Oscillation (MISO), has been the main focus of the research into the intraseasonal variability of the South Asian monsoon (e.g., Lawrence and Webster 2002). The variability on 10-20 day timescales, referred to as the Quasi-Biweekly Oscillation (QBW), has received somewhat less attention. Yet, the QBW explains, in a statistical sense, a high fraction of the monsoon rainfall variability (Chen and Chen 1993; Annamalai and Slingo 2001; Hoyos and Webster 2007).

Figure 1 shows, for boreal winter and summer, the climatological variance of Outgoing Long-wave Radiation (OLR; a proxy for convection) divided among three frequency bands. The variance for December to January is shown on the left column of Figure 1, while that for June to August is shown on the right. Over South Asia, the boreal summer 10-20 day band, associated with the QBW, explains a larger fraction of the variance than either the 20-30 and 30-60 day bands (i.e., compare Figure 1b to Figure 1d,f). Moreover, Figure 1 shows that the 10-20 day variance is mostly absent over South Asia during winter, shifting to the Southern Hemisphere, particularly to the northeast of Australia (Figure 1a).

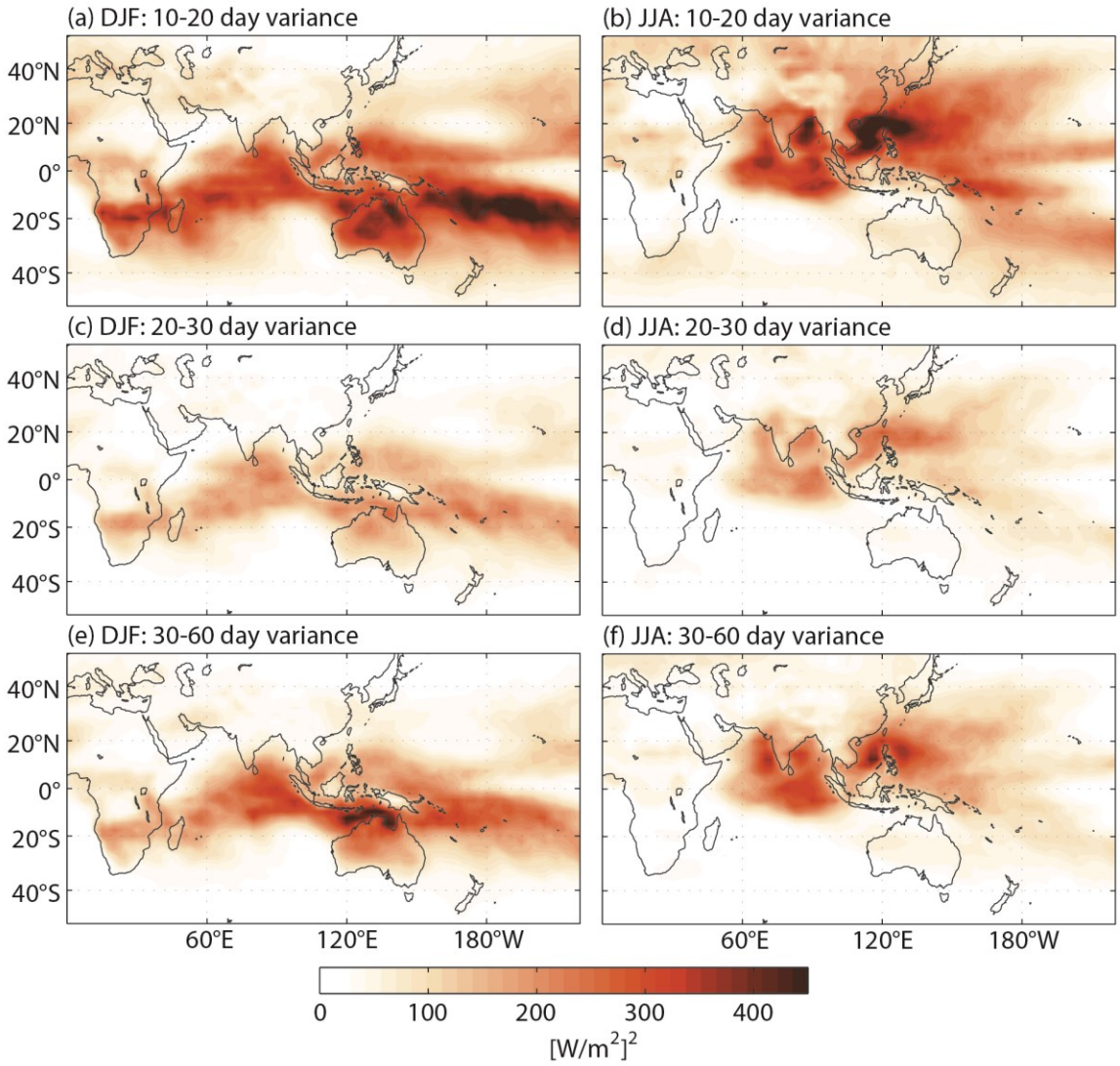

Figure 1 Climatological variance of the boreal winter (DJF; left column) and summer (JJA; right column) NOAA Outgoing Long Wave Radiation (OLR) for three different frequency bands. Notice the large amplitude of the summertime 10-20 day band over the South China Sea and the Bay of Bengal.

The typical QBW, as revealed by a composite analysis relative to minimum 10-30 day OLR averaged over the South China Sea, is shown in Figure 2. This analysis is consistent with Kikuchi and Wang (2009), who noted that the QBW is manifested as a synoptic scale convective anomaly with a periodicity of roughly two weeks. During the first seven days of the composite (Figure 2a,b,c) the QBW is apparent as a convective envelope (blue

shading on Figure 2) moving initially across the Philippines and later northwestward into the South China Sea. Then, during the last seven days (Figure 2d,e), the blue convective envelope drifts westward over South Asia, passing over the Bay of Bengal, India, and the Arabian Sea.

The track of the QBW over the West Pacific Ocean is reminiscent of the tropical cyclones that often develop over this region, and the track of the envelope over South Asia is reminiscent of the monsoon depressions that often develop over the Bay of Bengal (Sikka 1977; Saha et al. 1981; Krishnamurthy and Ajayamohan 2010; Hurley and Boos 2014). This is no coincidence, as studies show that the QBW, together with the MISO, modulate tropical cyclones (Li and Zhou, 2013) and monsoon depressions (Goswami 2003). Thus, a better understanding of the QBW might lead to an increased predictability of these weather systems.

Quasi-biweekly oscillations are also present in the upper troposphere over South Asia during the monsoon. The oscillations are observed in association with the monsoon anticyclone (Krishnamurti and Bhalme 1976; Wu et al. 2015), a planetary-scale feature with no counterpart on the globe, extending from the Pacific Ocean to Africa and from the Equator to about 40°N (Figure 3). The upper tropospheric oscillations can be seen, for instance, as westward moving anticyclones that repeatedly detach from the monsoon anticyclone (Popovic and Plumb 2001). We will refer to such upper troposphere oscillations, collectively, as the UQBW.

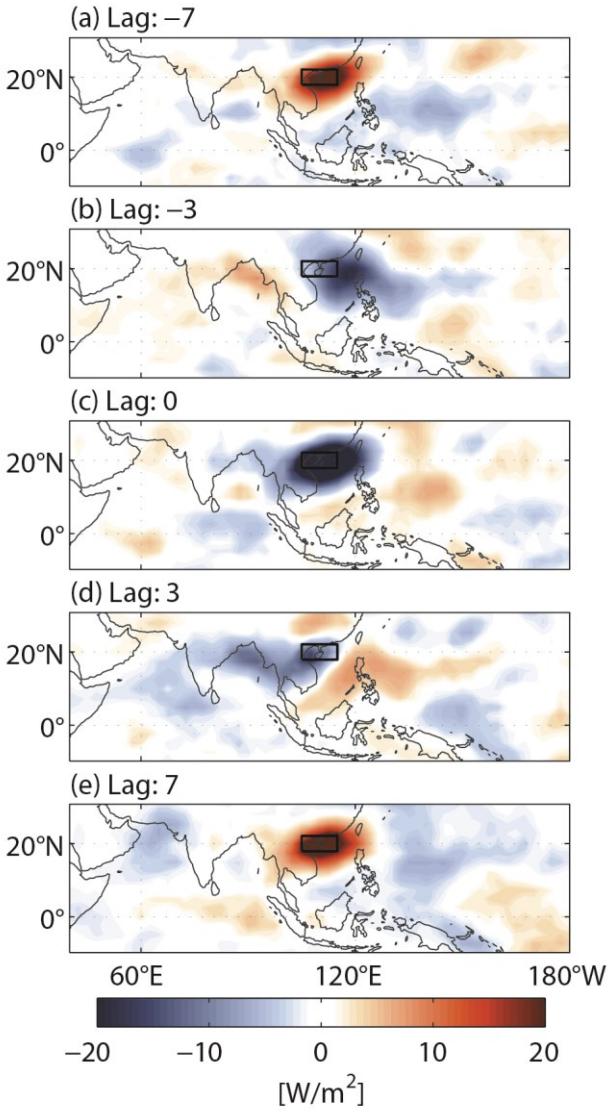

Figure 2 Composite of boreal summer (JJA) 10-30 day NOAA OLR relative to minimum values, that are less than one standard deviation, averaged over the South China Sea. The black box delimits the region over which OLR values were averaged to construct the composite.

Given the common timescale and location of the QBW and the UQBW, it is only natural to wonder if these two phenomena affect each other. In this study we provide insight into this question by focusing on the UQBW and its co-evolution with the QBW. We will show how the UQBW and the QBW fit together, emphasizing the upper tropospheric dynamics and, in particular, the phenomenon of Rossby-wave breaking.

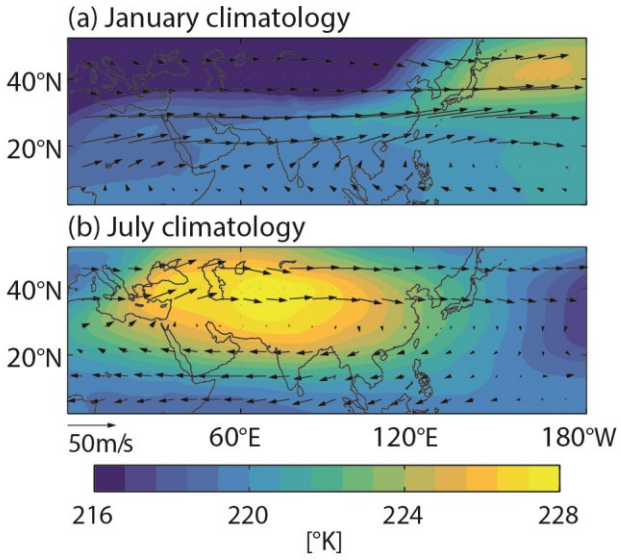

Figure 3 Climatology of the 200mb temperature field (shaded) and winds (arrows) for January and July. During January the upper level circulation is characterized by the subtropical jet stream, with westerly winds over the subtropics in response to a strong meridional gradient of temperature (a). In contrast, the circulation during July is characterized by the monsoon anticyclone, with winds circulating clockwise around a planetary-scale temperature maximum in the upper troposphere (b; yellow shading). The anticyclone is kept in place by the elevated sensible heating from the Tibetan Plateau and the diabatic heating due to convection (Hoskins and Rodwell 1995; Hoskins and Wang 2006; Wu et al. 2015). Data from the ERA-interim reanalysis.

In Section 2.2 we discuss the data and methods used in this study and briefly review some aspects of the potential vorticity (PV) framework (Hoskins et al. 1985) -- a framework that will be shown useful to understand the UQBW. In Section 2.3 we discuss general aspects of the upper tropospheric dynamics over South Asia as seen through its distribution of PV. In Section 2.4 we consider a case study that illustrates the sequence of events commonly observed for the UQBW and its co-evolution with the lower levels. In Section 2.5 we use a composite analysis to study the typical evolution of the UQBW and to reveal its co-evolution with the QBW. Finally, in Section 2.6, we discuss these results.

2.2 Data and methods

We use data from the ERA-interim reanalysis (Dee et al. 2011) to study dynamical and thermodynamical fields of the atmosphere on both the 370K isentrope and on pressure levels. Data on isentrope 370K is used to study the upper tropospheric levels over South Asia. Particularly, we study the 370K PV field, where the UQBW is readily identified. The isentrope is part of "middle world", meaning that it does not intersect the Earth's surface at any location and time (Hoskins 1991), and resides within the tropical tropopause layer (Fueglistaler et al. 2009). Its climatological height during January and July is shown in Figure 4, along with the height of several other isentropes.

PV is defined as

$$PV = \frac{1}{\rho}\boldsymbol{\omega} \cdot \nabla\theta \tag{1}$$

where ρ is the density of the air parcel, $\boldsymbol{\omega}$ its absolute vorticity, and $\nabla\theta$ the potential temperature gradient. For hydrostatic motion viewed in isentropic coordinates it takes the simpler form due to Rossby (1940):

$$PV = -g(\xi_\theta + f)\frac{\partial\theta}{\partial p} \tag{2}$$

where g is the acceleration due to gravity, ξ_θ the isentropic relative vorticity, f the Coriolis parameter, θ the potential temperature, and p the pressure field.

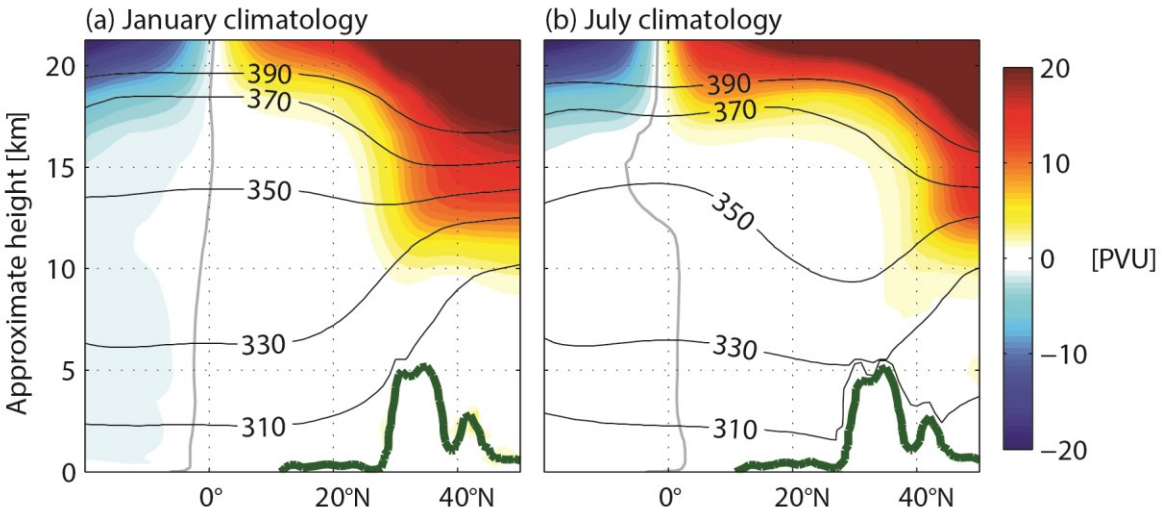

Figure 4 Climatology of potential temperature (black contours) and PV (shaded) averaged from 75E to 85E. PV is shown in Potential Vorticity Units (PVU= $10^{-6}\ m^2 \cdot s^{-1} \cdot K \cdot kg^{-1}$). The gray lines mark the zero line of PV. The green lines correspond to the 200K isentrope and mostly follow the surface. A scale height of 8 km was assumed to compute the approximate height. Data from the ERA-interim reanalysis.

Data on pressure levels is used to study the lower troposphere. Particularly, we study the 850mb geopotential height field and the Vertically-Integrated horizontal Moisture Transport (VIMT) following Fasullo and Webster (2003):

$$VIMT = -1/g \int_{p_s}^{p_t} q\boldsymbol{u}\, dp \qquad (3)$$

where $p_s = 1000$ hPa, $p_t = 300\ hPa$, g is the acceleration due to gravity, q the specific humidity, $\boldsymbol{u}$ the horizontal wind vector, and p the atmospheric pressure. Given the rapid decrease of specific humidity (q) with height, VIMT is strongly weighted toward transports in the lower troposphere. Additionally, we use NOAA Interpolated Outgoing Long-wave Radiation (OLR; Liebmann and Smith 1996) as a proxy for convection. All data is analyzed for the 1980 – 2013 period.

We use a simple 10-30 day top-hat filter for all fields in the analyses of Section 2.4 and 2.5, except where otherwise noted. Specifically, we remove unwanted temporal frequencies by using a rectangular function on the frequency domain. The filter isolates both quasi-biweekly oscillations, and the possible influence of other intraseasonal modes, while removing the high frequency components associated with the diurnal cycle and the low frequencies components associated with the annual cycle and the inter-annual modes. We test the statistical significance of the analyses of Section 2.5 by using a Monte Carlo technique (Livezey and Chen 1983).

2.2.1 "Potential Vorticity Thinking" in Tropical Dynamics

The use of 370K PV to study the UQBW is motivated by the ideas within the "PV-thinking" framework of Hoskins et al. (1985). For our purposes, there are three key ideas. First, the PV evolves simply by advection (i.e., it is conserved for each fluid parcel) whenever diabatic heating, and forces such as friction or gravity-wave drag, are negligible. In such circumstances one can easily track fluid parcels by studying the evolution of the PV field. This will allow us to characterize the UQBW life cycle more sharply, revealing that the UQBW is both a midlatitude and a tropical phenomenon. Second, in the tropical upper troposphere the main departure from advective evolution occurs when anticyclonic PV anomalies are created diabatically, for instance in cumulonimbus detrainment regions (Hoskins and Wang 2006). Such diabatic PV changes are the main reason for the existence of the monsoon anticyclone itself. Third, isentropic distributions of PV contain all relevant dynamical information when balanced dynamics is a good approximation of the particular case study; this idea is referred to as PV invertibility (e.g. Hoskins et al. 1985; Davis 1992;

McIntyre and Norton 2000). Thus, when applicable, PV invertibility allows the retrieval of the winds, temperature, and all other dynamical fields, from the knowledge of the PV field.

There is also an important limitation of PV-thinking that should be kept in mind; PV-thinking does not account for equatorial Kelvin waves as they are not balanced motions. So in the tropical atmosphere, where Kelvin waves are known to play an important role (e.g., in shaping the circulation; Gill 1980), PV-thinking alone cannot provide a full picture of the near-equatorial dynamics (Schubert and Masarik 2006). Yet, regardless of this limitation, PV-thinking has been shown to be particularly useful when considering interactions between the tropics and midlatitudes (e.g., Slingo 1998; Waugh and Polvani 2000; Knippertz 2007; Masarik and Schubert 2013), and it stands firmly as a useful diagnostic tool and as an important conceptual framework to understand the tropical atmosphere.

2.2.2 Extended Empirical Orthogonal Function Analysis

In Section 2.5 we conduct an Extended Empirical Orthogonal Function (EEOF) analysis following Weare and Nasstrom (1982) and Kikuchi and Wang (2009). The EEOF analysis makes use of the strong spatial and temporal correlation of geophysical fields to compute empirical functions that show their typical evolution. Our analysis differs only slighthly from the previous authors in that we use two different fields: 370K PV and OLR. That is, we construct a multivariate EEOF by using data from both the upper and lower tropospheric levels.

We consider 10-30 day fields (obtained by using the top-hat filter) and only use the values in-between May and September. We normalize each 10-30 day field, previous to the EEOF

analysis, by dividing each field by their saptially-avareged standar deviation. That is, the average of the standard deviations over all points for which the field is defined. This normalization prevents the relative magnitude of the fields from affecting the results of the analysis. We use 8 time increments of 2 days, therefore using a time period of 16 days for the EEOF analysis.

2.3 South Asian upper troposphere dynamics as seen through the 370K PV field

The annual cycle of the upper tropospheric levels, as seen through their PV and wind fields, reveals an interesting picture of the monsoon anticyclone and of its relation with the UQBW.

Consider the climatological 370K PV field for January and July as it is shown in Figure 5. Here the black arrows represent horizontal wind vectors on the 370K isentropic surface, the gray lines separate regions of easterly and westerly winds, and the shades represent the PV field; red for positive PV and blue for negative.

During January, the 370K PV field seems to increase monotonically with latitude at every longitude,[6] with a ridge east of Asia and a trough west of North America, over the Pacific Ocean, being its most prominent characteristics. At this time, strong westerly winds are present over Asia poleward of about 10°N, associated with the subtropical jet, and weak easterly winds are present equatorward of this latitude (Figure 5a).

[6]In reality there is a weak PV maximum near the equator, so that the statement is only an approximate one. The PV field seems to increase monotonically with latitude as a consequence of the color-scale we used, but if the figure where to be scaled so that its limits went from -4 to 4 PVU (saturating the colors in figure), then evidence of the weak PV maximum near the equator, extending from the East Pacific Ocean to the Arabian Sea, would be seen in the climatology. The presence of this PV maximum near the equator during boreal winter, however weak, has an impact on the circulation. The reason for its existence as well as its impacts on the circulation will be considered in a future paper.

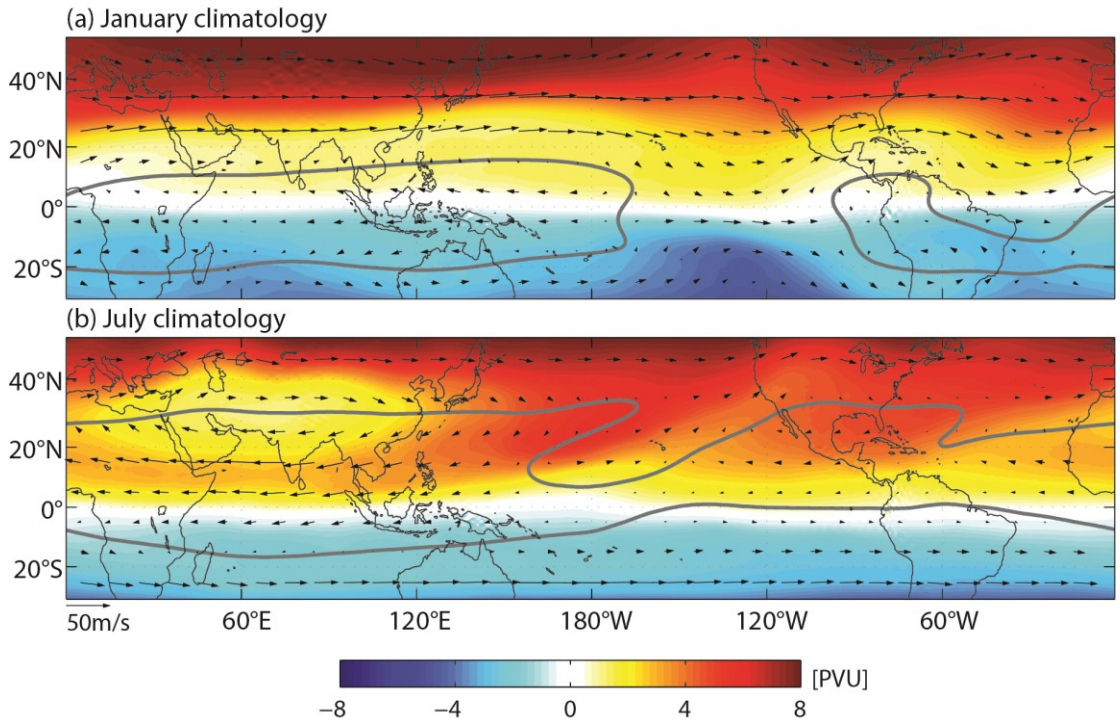

Figure 5 Climatology of the 370K PV field (shaded), the 370K isentropic winds (black arrows), and the boundary between westerlies and easterlies (gray contours) for January (a) and July (b). During July, the monsoon anticyclone is evident as a local minimum of the PV field centered over the Tibetan Plateau. Data from the ERA-interim reanalysis.

From February to June, the 370K PV field undergoes major changes. Between February and April, the trough west of North America gradually elongates southwestward, bringing midlatitude PV closer to the equator. From May to June, the establishment of the monsoon anticyclone becomes evident as small but positive values of PV develop over the Tibetan Plateau and midlatitude PV, associated with the PV through west of North America, tends to surround the anticyclone.

During July, at the peak of the monsoon season, midlatitude PV completely surrounds the anticyclone. At this time, the westerly winds over Asia have shifted northwards up to about 30°N and the easterly winds close to the equator, known at this time as the easterly jet stream, have intensified (Figure 5b).

Important changes are also observed in the zonal winds over the Pacific Ocean between January and July. While westerly winds are present over the east equatorial Pacific Ocean during January (Figure 5a), these move further north over the Pacific Ocean during July and a continuous band of easterly winds wraps around the equator (Figure 5b). The equatorial westerly winds present during January are known as the "westerly ducts" (Webster and Holton 1982), and are dynamically important in that they determine the regions where the tropics and midlatitudes can preferentially interact via Rossby-wave dynamics (Kiladis and Weickmann 1992; Tomas and Webster 1994; Waugh and Polvani 2000; Funatsu and Waugh 2008). The westerly winds during July have yet to be granted a name, but they seem to play a similar role during July to that of the westerly ducts during January. In fact, as we shall see, the regions where the tropics and midlatitudes can preferentially interact during the boreal summer seem determined by the presence of these westerly winds.

Figures 6 and 7 suggest that the PV feature that surrounds the monsoon anticyclone during July (Figure 5b) reflects the presence of the UQBW. Figure 6 shows Hovmöller diagrams of the 370K PV field averaged across three different latitude bands, all located on the equatorward side of the anticyclone. A marked transition occurs between winter, when relatively high PV propagates eastward, and summer season, when the anticyclone is present and high PV propagates westward. Figure 7 shows the climatological summertime variance of the 370K PV field divided among three intraseasonal frequency bands. It suggests, by comparing the three panels of Figure 7, that the summertime transients have a strong quasi-biweekly component. Thus, we identify the positive PV that propagates

westward during summer (Figure 6) with the UQBW, and note that the UQBW is a recurrent phenomenon, manifesting itself several times during the boreal summer.

In the next sections, we show that the UQBW is related with a distinct sequence of events. The UQBW appears first as a midlatitude Rossby wave and latter transitions into a PV anomaly advected around the monsoon anticyclone. Such transition implies the *breaking* of such wave; a breaking that can be thought of as the irreversible deformation of the PV contours previously associated with wavelike motions (i.e., reversible undulations of the PV contours; McIntyre and Palmer 1983). In other words, the breaking occurs when the displacement of PV contours is such that the induced circulations leads not to the propagation of Rossby waves but to irreversible displacements, possibly leading to mixing of PV along isentropes, strongly modifying the wave dynamics, and leaving behind PV anomalies that can be tracked back to the wave-breaking event.

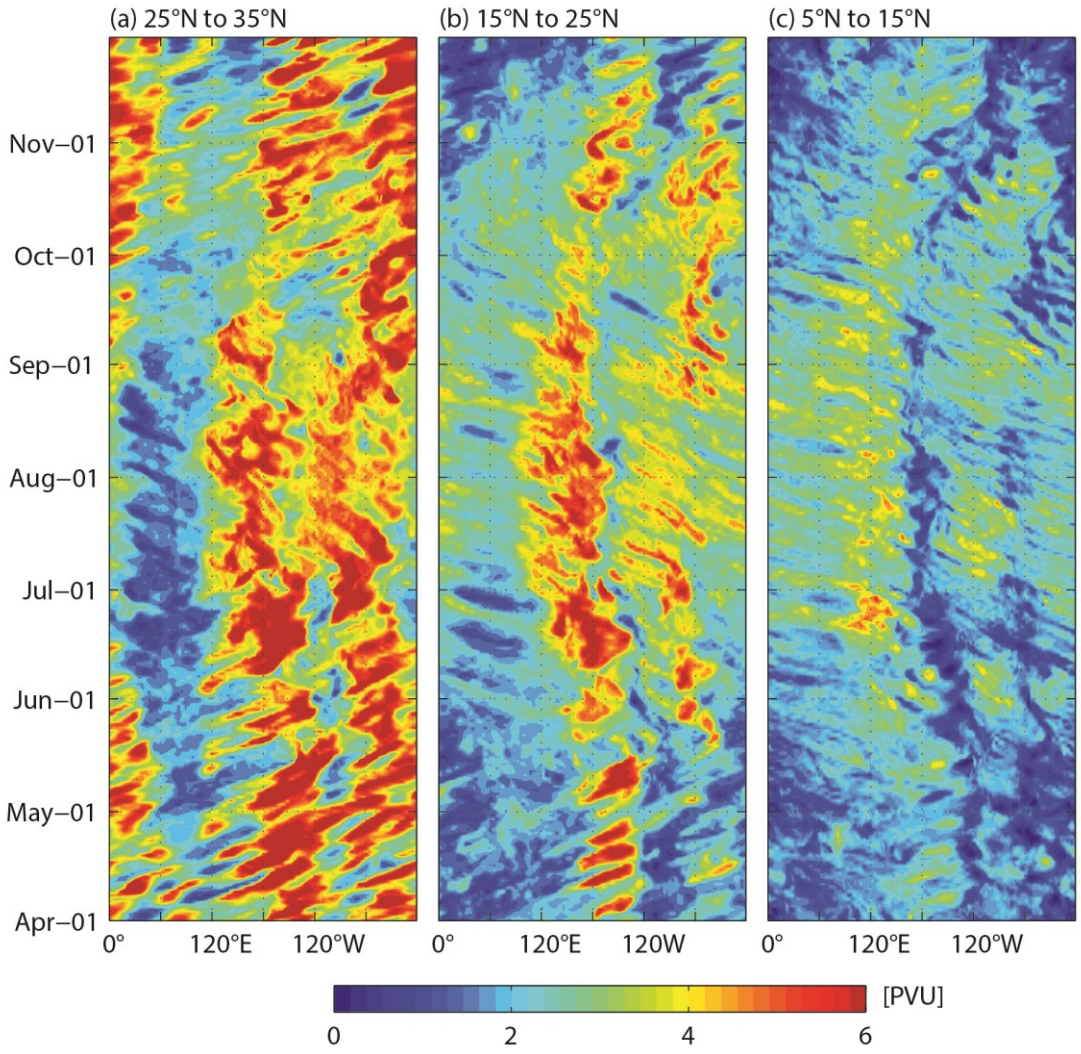

Figure 6 Hovmöller diagram of the 370K PV field averaged from (a) 25N to 35N, (b) 15N to 25N, and (c) 5N to 15N during 2008. Data from the ERA-interim reanalysis.

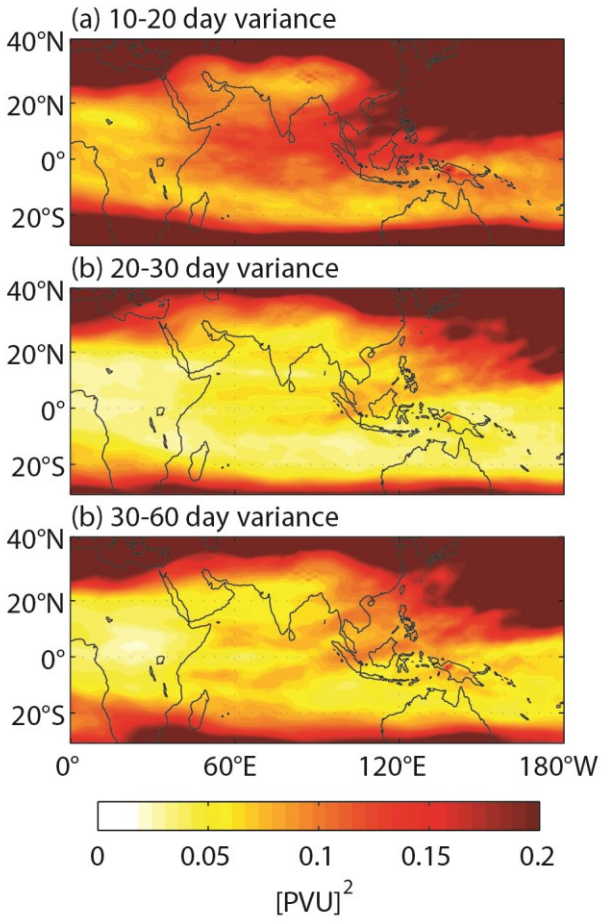

Figure 7 Climatological variance of the summertime (JJA) 370K PV field for three different frequency bands. Data from the ERA-interim reanalysis.

2.4 Case Study: An event of maximum 370K PV over India

We characterize the UQBW with an index based on the 370K PV field over India. The index is defined as the time series of the 10-30 day PV field averaged over a box that extends from 5° to 20° North and from 70° to 90° East (Peninsular India; black box on Figure 9), which is then normalized by subtracting its mean and dividing by its standard deviation. We use a Lanczos filter (Duchon, 1979), as opposed to the top-hat filter discussed in Section 2.2, to compute this index. The location of the box is chosen both because it is on the southern edge of the monsoon anticyclone and because the 370K PV

over the box exhibits significant power in the 10-20 day band (Figure 7). Thus, we expect the index to capture the variability of the UQBW.

Additionally, events of maximum 370K PV over India, referred to hereafter as MPV events, are defined as those days in between May and September for which the index is above 1.5 standard deviations, corresponds to a local maximum, and is at least 5 days apart from other MPV events. Defined this way, we obtain a total of 132 MPV events for the 34 years analyzed of the ERA-interim reanalysis, an average of about 4 events per season (May to September). Their temporal distribution is shown in Figure 8, revealing a marked increase in the percentage of MPV events from June (14% of the events studied) to July (27%), and slightly lower percentages thereafter for August (23%) and September (22%).

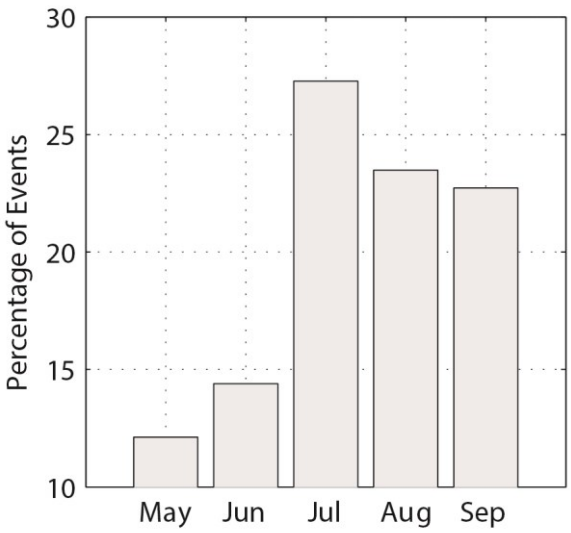

Figure 8 Percentual distribution of MPV events during the period of study (from 1980 to 2013). Data from the ERA-interim reanalysis.

In this section we focus on just one of these MPV events, that of June 22, 2008. This particular event is chosen as it was the strongest one observed in the ERA-interim reanalysis (i.e., it had the largest 370K PV index), and because both the lower and upper

tropospheric fields resemble the composite of the MPV events. Yet, it should be kept in mind that deviations from the averaged behavior are certainly possible and perhaps common, so that the correlations between the upper and lower tropospheric fields might not be as evident, in other events, as in this particular case.

Figure 9 shows the 370K PV field (left column) and its 10-30 day anomalies (right column) around the MPV event of June 22, 2008. The dates range from nine days before the event, to six days after, at three-day increments. Thus, the sequence of events associated with the UQBW can be easily followed.

From June 13 to 16, a midlatitude wave appearing as a trough on the PV field propagates eastward from the Sea of Japan to the North Pacific Ocean (Figures 9a,c). The propagation is seen in the 10-30 day PV field as a positive anomaly over the Sea of Japan (Figure 9b) that moves to a position east of Japan by June 16 (Figure 9d). By June 19 the wave trough has elongated equatorward, with its thinned trough reaching as far as 10°N (Figures 9e,f). Moreover, by this time the PV trough has a southwestward orientation, indicative of a Rossby wave-breaking event of the kind pointed out by McIntyre and Palmer (1983).

On June 22 the trough has lost its coherence, perhaps because of another wave-breaking event over the Central Pacific (Figure 9g). Yet, the signal can still be traced within the 10-30 day PV field as a positive anomaly circling the upper level anticyclone in a clockwise direction: stretching from the North Pacific Ocean, southeast of Japan, and passing the Philippines, the Gulf of Thailand, the Bay of Bengal, Peninsular India, and terminating over the Arabian Sea and Africa (Figure 9h). By June 25, the PV anomaly has moved further west to the Red Sea (Figures 9i,j); again, following a path around the anticyclone.

Finally, by June 28, the PV anomaly appears to have been partially recirculated back into the midlatitudes (Figures 9k,l), and the upper tropospheric field returns close to its initial state.

Changes in the VIMT and the 850mb geopotential field are observed in synchrony with the 370K PV anomalies associated with the UQBW. We will focus on the changes over the West Pacific Ocean and South Asia. Figure 10 shows both the unfiltered VIMT (left column), and the 10-30 day 850mb geopotential (right column), for the same period as that of Figure 9.

From June 13 to 16, a positive geopotential anomaly moves eastward from the Korean Peninsula to Japan, reaching south as far as to the Philippines on June 16 (Figures 10b,d), and displaying a similar behavior to the positive 370K PV anomalies to their east (Figures 9b,d). Over South Asia, a negative geopotential anomaly and a strong VIMT towards the continent are present during these same days (Figs 10a to 10d).

By June 19, the positive geopotential anomaly that propagated eastward over the Korean Peninsula has moved further east, and displays a southwestward orientation that stretches from the North Pacific Ocean to the Bay of Bengal (Figure 10f). The orientation of the anomaly is reminiscent of the positive anomalies on the 370K PV field (Figures 9e,f). Additionally, the VIMT towards South Asia has weakened considerably (Figure 10e).

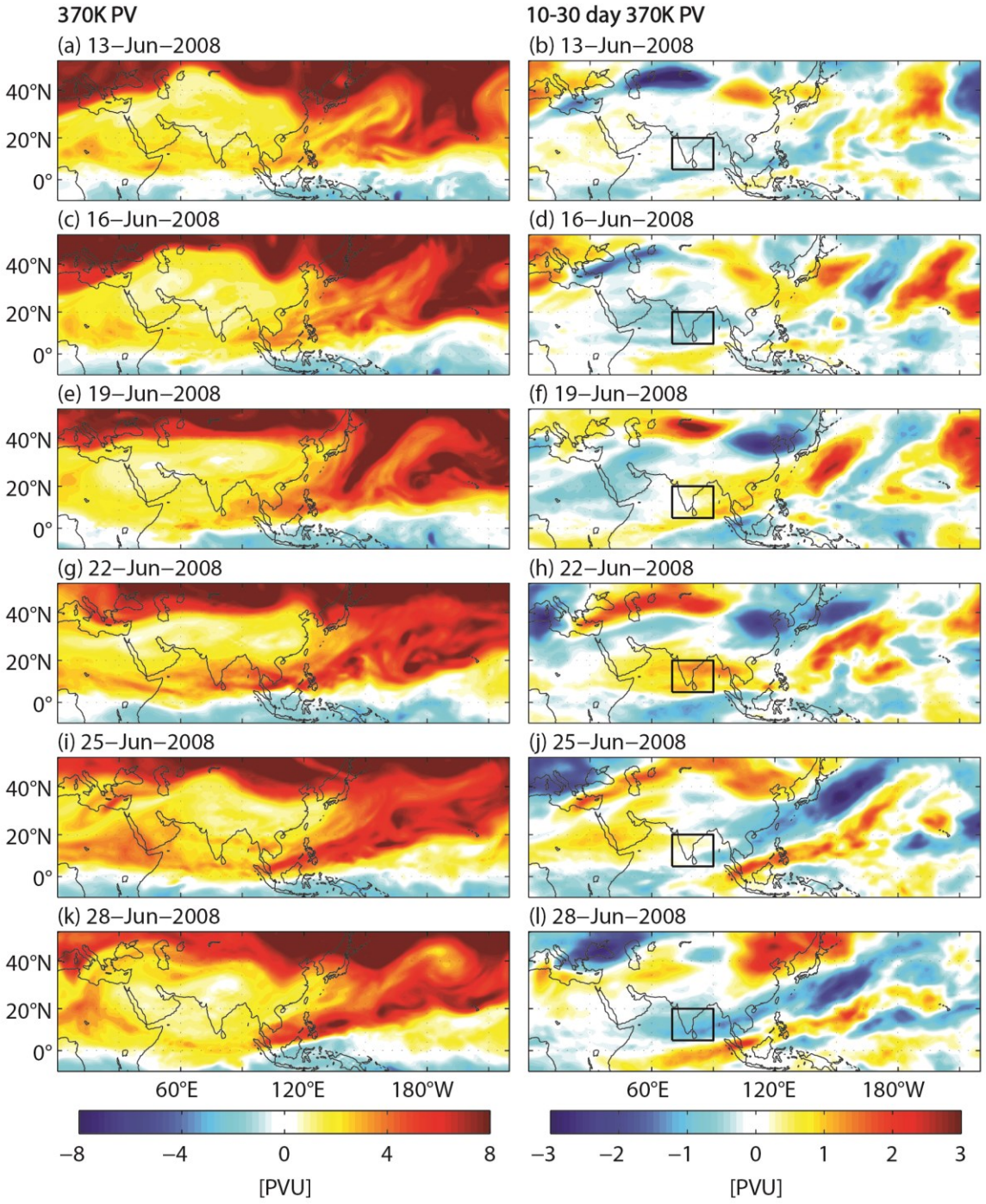

Figure 9 Evolution of the 370K PV field (left column) and its 10-30 day anomalies (right column) around the MPV event of June 22, 2008. The black box delimits the region over which the 10-30 day PV anomalies were averaged to define the MPV events. Data from the ERA-interim reanalysis.

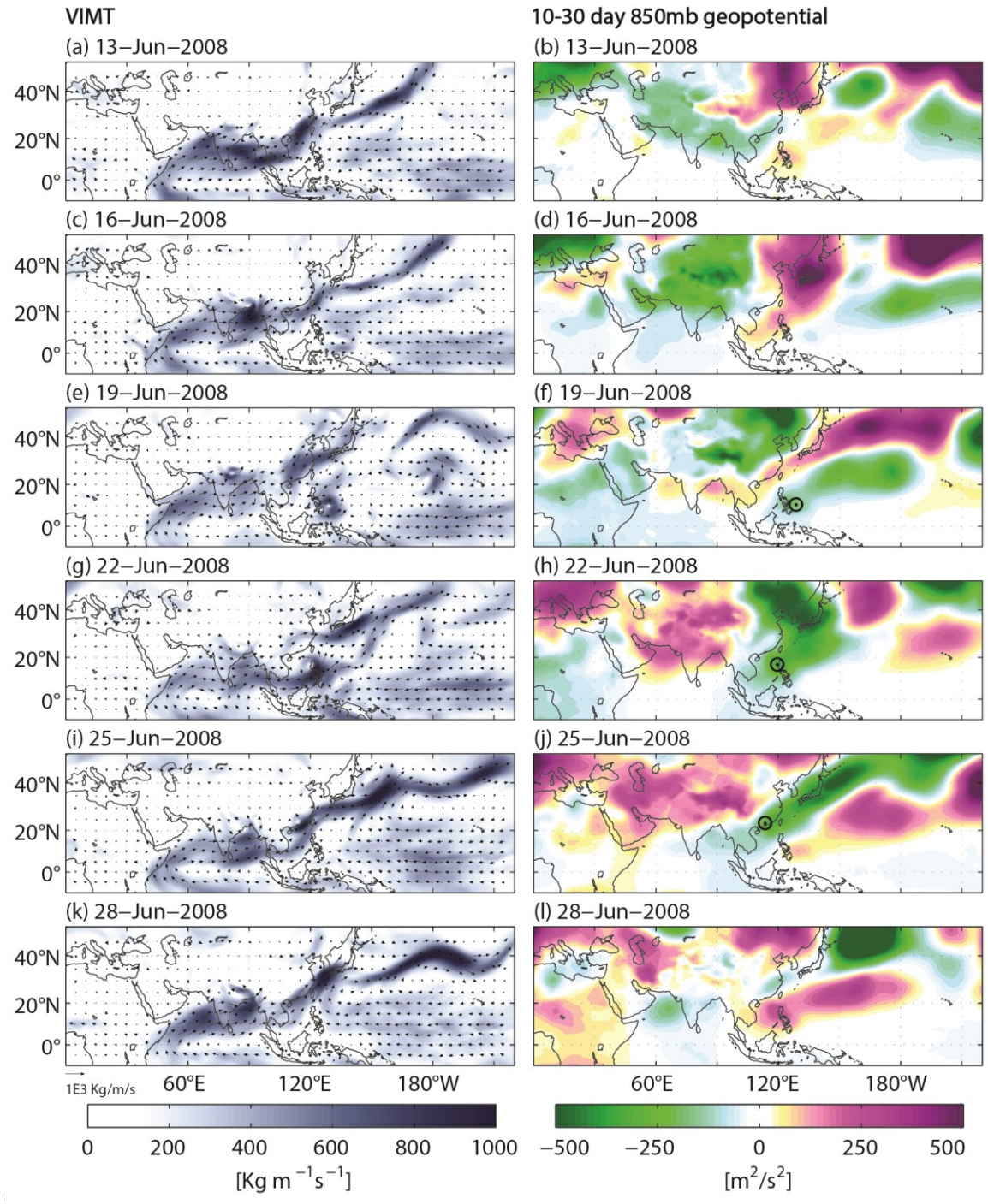

Figure 10 Evolution of the full VIMT field (left column) and the 10-30 day 850mb geopotential anomalies (right column) around the MPV event of June 22, 2008. Typhoon Fengshen location, for the days that it was either a tropical depression or a stronger system, is marked with a black circle on the right column panels. The location was retrieved from NOAA's real-time tropical cyclone products website (http://rammb.cira.colostate.edu/products/tc_realtime). All other data was retrieved from the ERA-interim reanalysis.

On June 22, the day of the MPV event, a positive geopotential anomaly is still present over South Asia and the VIMT towards South Asia remains weak (Figures 10g,h). The positive geopotential anomaly seems to have evolved from that of previous days, but it has now spread over a much wider region.

On June 25, a negative geopotential anomaly reaches South Asia (Figure 10j) and the VIMT over the Bay of Bengal strengthens (Figure 10i). The negative geopotential anomaly stretches from northeast of Japan to the Bay of Bengal (Figs 10j) with an orientation that is reminiscent of a negative anomaly on the 370K PV field (Figure 9j). The negative geopotential anomaly can be tracked from June 13 beginning over the center Pacific Ocean, near Hawaii; moving westward until it reaches the Philippines on June 19, and then northwestward until it reaches Hong Kong on June 25. Finally, by June 28, the lower tropospheric fields return close to their initial states (Figure 10k,l).

We note that the MPV event coincides with the time when Typhoon Fengshen (also known as Typhoon Frank) was active over the Philippines. Fengshen was first identified as a tropical depression just north of Palau on June 17, transited over the Philippines from June 20 to the 22, and reached Hong Kong on June 25 (Gutro, 2008). Fengshen proved to be particularly hard to predict and had a devastating impact over the Philippines and China (Gutro, 2008). Fengshen's location, for the days that it was a tropical depression or as a stronger system, is marked with a black circle on the right column of Figure 10.

2.5 Composite features of the UQBW and its co-evolution with the QBW

A lagged composite of the 10-30 day 370K PV field, relative to the MPV events, illustrates the typical life cycle of the UQBW through the progress of positive PV anomalies (Fig 11; left column).

Seven days before the MPV event, at lag -7, two positive PV anomalies are situated over midlatitudes (Figure 11a). One of these anomalies starts close to Beijing and moves eastward, while the second one is observed over the North Pacific Ocean, west of Japan, moving slowly southward (Figs 11a,c). At lag -5, after the eastward moving anomaly has reached the North Pacific Ocean, an elongated positive PV anomaly stretches from the North Pacific Ocean to Malaysia in a path around the upper level anticyclone (Figure 11c). The southwestward orientation of the anomaly is the result of individual Rossby wave-breaking events and the advection of their related PV by the anticyclone. From lag -5 to lag +2 the positive PV anomaly continues moving on a path around the anticyclone. It moves from the North Pacific Ocean to northwest Africa (Figures 11c,e,g,i), transiting India at lag 0 (Figure 11g). Finally, at lag +5, the positive PV anomaly is situated on the western flank of the anticyclone propagating northward, thus indicating a recirculation of PV to midlatitudes (Figure 11k).

Co-occurring with the UQBW, statistically significant dynamic and thermodynamic anomalies are also observed in the lower troposphere. Composites of 10-30 day VIMT, 10-30 day 850mb geopotential, and 10-30 day OLR, relative to the dates of the MPV events, are shown on the right-hand column of Figure 11 and illustrate this co-occurrence.

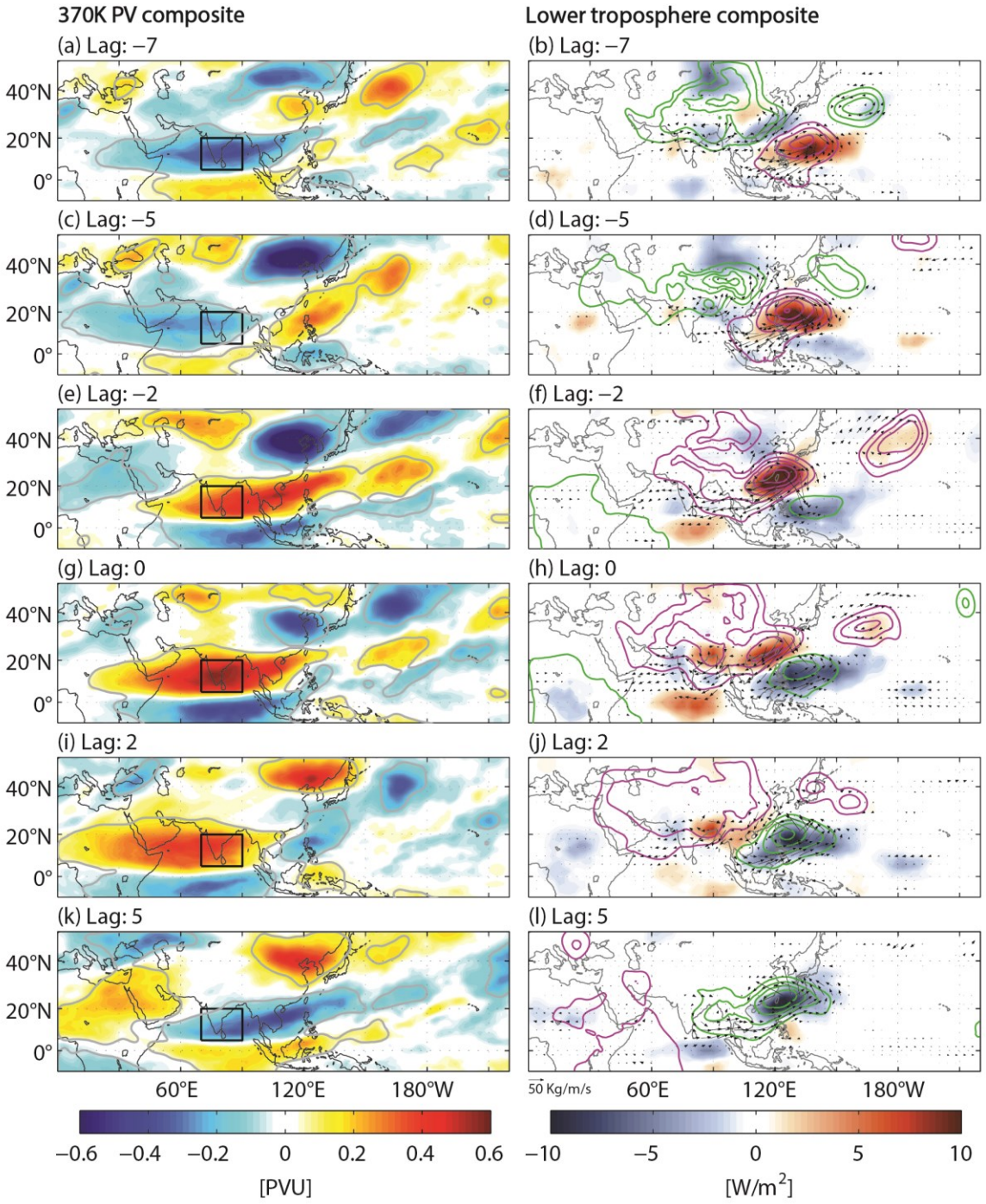

Figure 11 Composites of upper (left column) and lower tropospheric fields (right column) relative to MPV events. Shades on the left column represent 10-30 day 370K PV anomalies, and the gray contours represent the 95% level of statistical significance. The black box delimits the region over which the 10-30 day PV anomalies were averaged to define the MPV events. Shades on the right column represent 10-30 day OLR anomalies; positive (red) values correspond to suppressed convection. Green contours represent negative 10-30 day geopotential anomalies, starting at -10m^{2}s^{-2} and increasing by -30 m^{2}s^{-2}. Purple contours represent positive geopotential

anomalies, starting at 10 m^2s^{-2} and increasing by 30 m^2s^{-2}. Black arrows represent 10-30 day VIMT anomalies. The lower tropospheric fields are significant to a 95% level. All data, except for the NOAA OLR field, was retrieved from the ERA-interim reanalysis.

Consider, for instance, the weak lower tropospheric anticyclonic anomaly that at lag -7 is situated over the Philippine Sea (Figure 11b). The anticyclonic anomaly is evident as a positive anomaly in the 10-30 day 850mb geopotential (purple contours), as a positive anomaly in the 10-30 day OLR (red shades), and as an anomalous southward transport of moisture in the 10-30 day VIMT (black arrows); consistent with suppressed convection over the Philippine Sea. The anomaly moves northwestward from lag -7 to lag -2, gradually intensifying until it reaches the South China Sea (Figures 11b,d,f). From lag 0 to lag +2, the anticyclonic anomaly moves westward over South Asia, although with a weaker amplitude (Figures 11h,j). Finally, at lag +5, there are no longer significant signs of the anticyclonic anomaly, but a strong cyclonic anomaly (blue shades, green contours) now sits over the South China Sea (Figure 11l).

A co-evolution occurs between the upper and lower troposphere. A comparison between the left- and right-hand columns of Figure 11 reveals that the anticyclonic lower troposphere anomalies often sit below, or close to, positive 370K PV anomalies, with the opposite happening for cyclonic anomalies. This co-evolution is roughly maintained through the complete cycle of the UQBW, especially over the Pacific Ocean.

Moreover, it is important to note that the propagation characteristic and the temporal and spatial scales of the lower level anomalies correspond the QBW (e.g., Kikuchi and Wang 2009; Figure 2). This is significant as the composites were constructed relative to an index designed only to capture the variability of the UQBW. Therefore, the results suggest a co-

evolution of the UQBW and the QBW and, therefore, a co-evolution of the lower and upper troposphere. As Figure 12 reveals, this co-evolution also extends throughout the atmospheric column.

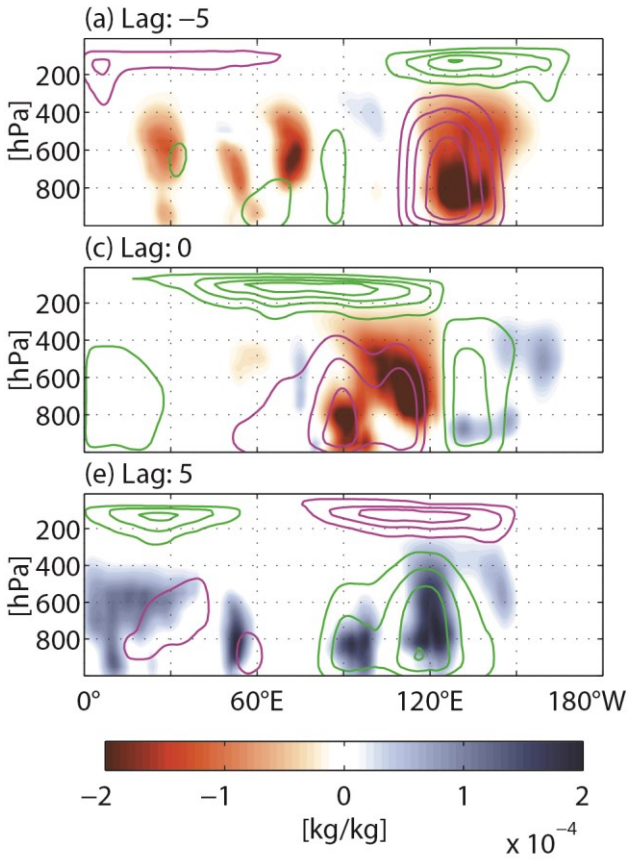

Figure 12 Composites of 10-30 day geopotential anomalies (contours) and 10-30 day specific humidity anomalies (shading) averaged from 10N to 25N, relative to MPV events. Green contours represent negative geopotential anomalies, starting at -10 m^2s^{-2} and increasing by -20 m^2s^{-2}. Purple contours represent positive geopotential anomalies, starting at 10 m^2s^{-2} and increasing by 20 m^2s^{-2}. All fields are statistically significant to a 95% confidence level. Data from the ERA-interim reanalysis.

To test this co-evolution hypothesis further, we carried out the multivariate EEOF analysis of both 10-30 day 370K PV and 10-30 day OLR discussed in Section 2.2. The full cycle of the first empirical orthogonal function of the EEOF analysis is show in Figure 13, where it is clear that the cycle corresponds to the co-evolution of the QBW and the UQBW, and

that the results agree with those found with the composite analysis; having a similar co-evolution of the upper and lower troposphere. The analysis reinforces the observational hypothesis that there is a strong correlation between the UQBW and the QBW.

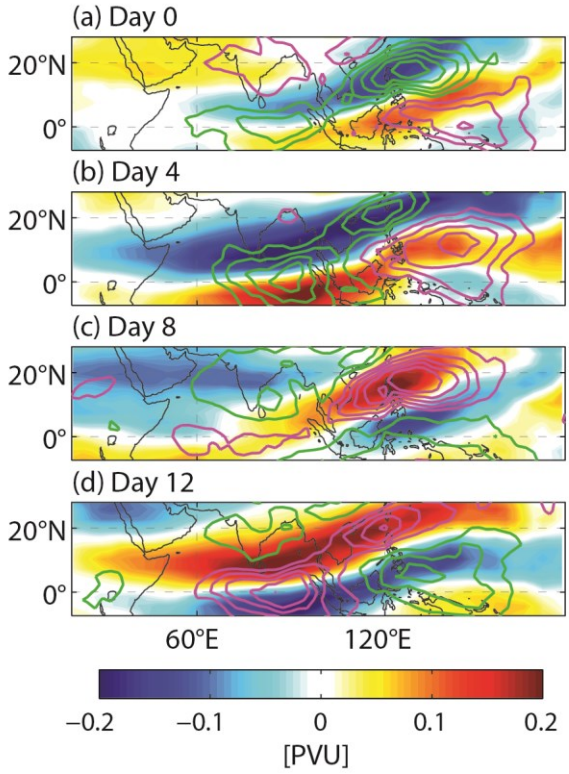

Figure 13 EEOF analysis for 10-30 day 370K PV (shaded) and 10-30 day NOAA OLR (contours). Green contours represent negative OLR anomalies starting at, and increasing by, -2 W/m^2. Purple contours represent positive OLR anomalies starting at, and increasing by, 2 W/m^2. The cycle represents the first EEOF of the analysis, the second EEOF exhibits an almost identical relationship between the 10-30 day 370K PV and 10-30 day OLR, together they explain 5.6% of the total variance. The 370K PV field was retrieved from the ERA-interim reanalysis.

2.6 Discussion

In this study we considered the UQBW and its correlation with the lower tropospheric QBW. We showed that the UQBW is a recurrent feature of the upper troposphere, occurring as long as there is a planetary-scale monsoon anticyclone; that a typical UQBW undergoes a distinct sequence of events that can be tracked on the 370K PV field; and that

the UQBW co-evolves with the QBW. Therefore, the study served to widen the picture of the quasi-biweekly oscillations of the South Asian monsoon by fitting together the lower and upper tropospheric variability.

Additionally, the case study centered around the MPV event of June 22, 2008, serves to point out the importance of studying the quasi-biweekly oscillations of the monsoon. The case study displayed similar correlations, between the upper and lower troposphere, to those found in the composites of Section 2.5 and its corresponding MPV event coincided with typhoon Fengshen transiting the Philippines.

2.6.1 The physical link between the UQBW and the QBW

Some studies suggest that the QBW causes the UQBW and discard the possibility that the UQBW might have an effect, however small, on the QBW. For instance, Randel and Park (2006) showed that deep convection over South Asia within a 10-20 day timescale is usually observed before an intensification of the monsoon anticyclone triggers the UQBW. Yet, they did not discuss the possibility that the UQBW might in turn affect deep convection. Hsu and Plumb (2000) and Popovic and Plumb (2001) noted the small vertical extent of the UQBW, and suggested that it was unlikely that the UQBW could affect the lower troposphere.[7] Additionally, the studies of Goswami and Mathew (1994) and

[7] This last argument is based on the ideas of PV invertibility for balanced motion. Studies of PV invertibility show that an upper-tropospheric PV anomaly with horizontal length-scale L induces wind and temperature fields that decay exponentially downward with an e-folding height scale of the order of the Rossby height, fL/N, where f is the Coriolis

Chatterjee and Goswami (2004) suggest that the QBW is as a response to the local dynamics of a moist tropical atmosphere, thus suggesting that the QBW is independent of the UQBW.

However, Figure 11 suggests that the UQBW affects the QBW and that perhaps they are a coupled phenomenon. The composite shows that deep convection over the South China Sea, associated with the QBW, generates anticyclonic circulations in the upper troposphere, reinforcing the monsoon anticyclone, and displacing PV northwards. This northward displacement of PV generates Rossby waves that travel eastward on the subtropical jet and break over the north Pacific Ocean. The PV associated with the breaking waves is then pulled towards the equator by the monsoon anticyclone and advected around the anticyclone in a Rossby-wave-breaking pattern. Importantly, when the Rossby waves break over the north Pacific Ocean, deep convection is observed over the Philippine sea. This convection is associated with a new cycle of the QBW; moving northwestward while intensifying and reaching the South China sea after 10 days. Thus, the composite analysis show that the UQBW is observed after deep convection is seen over the South China sea, but also show that deep convection reaches once again the South China sea 10 days after the UQBW is observed as a breaking Rossby wave.

---

parameter and N is the buoyancy or Brunt–Väisälä frequency (see Hoskins et al. 1985, Eq. 33c). Following this argument, thin upper-tropospheric PV anomalies over tropical regions, such as those associated with the UQBW, are not expected to greatly affect the lower-tropospheric levels.

Other studies also suggest an effect of the upper tropical troposphere on the lower troposphere. Koteswaram and George (1957) suggested that upper tropospheric circulation anomalies traveling westward on the easterly jet over South Asia affect the formation of monsoon depressions over the Bay of Bengal. Sadler (1976) described the development of three typhoons while an upper tropospheric trough, that we identify with the UQBW, was present over the Pacific Ocean. Sadler further hypothesized that the upper level trough could have affected the developing typhoons by decreasing the vertical wind shear and increasing the upper tropospheric divergence. Similar mechanisms might explain the co-evolution we observe between the UQBW and the QBW.

Moreover, modeling studies of the UQBW might help explain the timescale of the QBW (e.g., Murakami and Frydrych, 1974; Hsu and Plumb, 2000; Liu et al., 2007). In particular, the modelling study of Liu et al. (2007) suggests that the UQBW, and its timescale, are independent of the QBW. Liu et al. considered a global primitive equation model, and forced a monsoon anticyclone on it by using a time-independent diabatic forcing. The model anticyclone developed quasi-biweekly oscillations in the upper troposphere (i.e., the model's UQBW) without any representation of the lower tropospheric QBW. Thus, their study makes it reasonable to hypothesize that the timescale of the QBW is affected by that of the UQBW.

It is then important to establish if better predictability of tropical weather systems, such as typhoons and monsoon depressions, can be obtained by an improved knowledge of the upper level intraseasonal oscillations such as the UQBW. Our study suggests that this might be the case.

2.7 Acknowledgements

We thank the two reviewers for their thoughtful and careful reviews of the paper and their suggestions regarding the analyses. We thank the second reviewer especially for his comments on style and presentation that we feel has increased considerably the lucidity of our arguments. We also thank Professor Sir Brian Hoskins and Professor Judith Curry for their helpful suggestions during the course of this research project. Funding support for this research was provided by the Climate Dynamics Division of the National Science Foundation under Grant NSF-AGS 0965610.

CHAPTER 3. THE EFFECT OF POTENTIAL VORTICITY FLUXES ON THE TROPICAL UPPER TROPOSPHERE

Sebastián Ortega, Peter J. Webster, Violeta Toma, Hai-Ru Chang
This work is in preparation and will be submitted to the Journal of Atmospheric Science.

3.1 Introduction

From a climatological perspective, three major features dominate the upper tropical troposphere: westerly jet streams, upper tropospheric easterly winds, and "westerly ducts[8]" (Figure 14a,b). The jet streams are bands of strong westerly winds over the subtropics (Krishnamurti 1961). The upper tropospheric easterly winds are regions of easterly winds, in between the jet streams, that tend to extend around the entire tropics. And the westerly ducts (Tomas and Webster 1994; Webster and Holton 1982) are regions of westerly winds that separate or intrude the upper tropospheric easterly winds.

These three features display a strong annual cycle, yet they remain identifiable, in different forms and locations, throughout the year. Take the northern hemisphere as an example: when going from boreal winter to summer the westerly jet stream weakens and moves northward, the westerly ducts does just the same, and the upper tropospheric easterlies

[8]In the current literature, the term "westerly ducts" is used exclusively for the westerly winds present over the equatorial Pacific and Atlantic during boreal winter (Webster and Holton 1982). However, we will use the term, both during boreal summer and boreal winter, for the westerly winds close to or over the equator.

change from a region of easterly winds that tends to extend around the tropics, to one that completely surrounds it, with easterly winds that are particularly strong over the Indian Ocean, known as the easterly jet (Koteswaram 1958). Moreover, the northward displacement of the subtropical westerly jet, and the intensification of the equatorial easterly winds, reflect the formation of the monsoon anticyclones over Asia and North America, as described by Ortega et al. (2016) and as it is evident in Figure 14b.

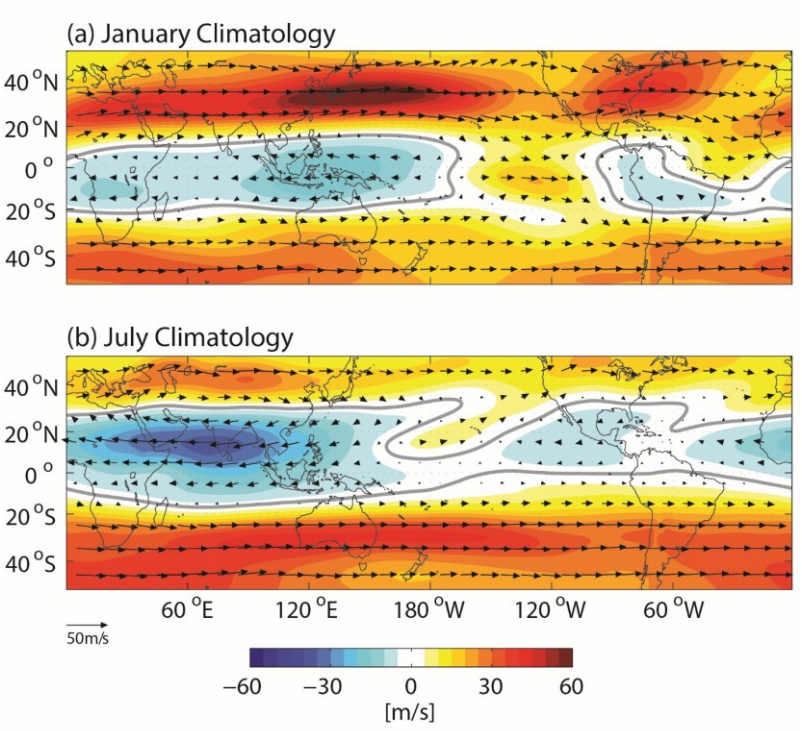

Figure 14 Climatological winds (black arrows) and zonal wind speed (shades) on the 370K isentrope. ERA-Interim data.

The distinction of these three upper tropospheric circulation features, while may seem arbitrary, is useful. The choice is based on the different dynamical processes that occur. Within the westerly jet streams Rossby waves constantly propagate eastward relative to the Earth (Chang and Yu 1999). Within the westerly ducts these Rossby waves move

equatorward and break[9] (Kiladis and Weickmann 1992; Knippertz 2007; Ortega et al. 2016; Postel and Hitchman 1999; Slingo 1998; Tomas and Webster 1994; Waugh and Polvani 2000). And within the equatorial easterly winds, upper tropospheric eddies, formed as by-products of the Rossby wave-breakings, are transported westward near the equator and slowly northward back towards the subtropical westerly jet (Koteswaram and George 1958; Ortega et al. 2016; Slingo 1998).

In this paper we explore the dynamics that support these circulation features, and discuss how they are formed, maintained, and how they interact. We show that these features are intimately linked, so that they cannot not be considered in isolation. In particular, we suggest that the westerly ducts are an integral response of the upper tropospheric circulation to very basic first order physics. Furthermore, we suggest that it is not possible to explain the basic state of the tropical atmosphere, even in an aqua-planet system, by considering zonally symmetric physics alone.

In Section 3.2 we review the data, the methods, and the concepts that will be used in this study. In Section 3.3 we revisit the large-scale circulation features of the upper troposphere as seen through its potential vorticity (PV) field. In Section 3.4, we present an analytical argument suggesting that meridional PV fluxes should always be expected in the topical upper troposphere and that imbalances in these fluxes help maintain the upper tropospheric

[9] The breaking of Rossby waves should be understood in the sense discussed in McIntyre and Palmer (1987). A Rossby wave is said to break when potential vorticity contours, which sustain the wave, are irreversibly deformed, leading to the mixing of the potential vorticity field instead of the propagation of the wave.

circulation. In Section 3.5, we explore these ideas for two different simulations of a shallow water model. Finally, we discuss results in Section 3.6.

3.2 Data and Methods

We use daily averages of the ERA-interim reanalysis data set (Dee et al. 2011) on isentropic surfaces. In particular, we use the PV and wind fields on the 370K isentrope, which in the tropics is close to the tropopause, to study the large-scale circulation of the upper troposphere. And we also consider isentrope 330K, which is close to the 500mb level, to study the large-scale circulation of the mid-tropospheric levels.

We use a shallow water model to study the effects that its PV fluxes have in its circulation and to gain insight into the effect that upper tropospheric PV fluxes might have on the tropical atmosphere. The model is described in Arakawa and Lamb (1992) and solves the momentum and mass conservation equations in a beta plane. The equations can be written as

$$\frac{\partial \boldsymbol{v}}{\partial t} - qh\boldsymbol{k} \times \boldsymbol{v} = -\nabla[K_E + gh] - k\boldsymbol{v} \tag{4}$$

$$\frac{\partial h}{\partial t} + \nabla \cdot (h\boldsymbol{v}) = S \tag{5}$$

where $\boldsymbol{v}$ is the wind vector, $q = \eta/h$ is the potential vorticity of the flow, η the absolute vorticity, h the depth of the shallow field, $K_E = |\boldsymbol{v}|^2/2$ the kinetic energy of the flow, g the acceleration due to gravity, k a linear damping term, and S a mass source-sink term. We define S as a relaxation towards an equilibrium height h_e within a timescale τ as in Hsu and Plumb (2000):

$$S = \frac{(h - h_e)}{\tau} \tag{6}$$

The source term S is intended to represent the effect of convection on the upper troposphere. And we define the equilibrium height (h_e) following Webster and Chang (1988):

$$h_e = H + A \exp\left\{ - \left| \frac{\lambda - \lambda_0}{\sigma_\lambda} \right| - \left(\frac{\phi - \phi_0}{\sigma_\phi} \right)^2 \right\} \tag{7}$$

where H is a reference height and set to 500m for this study, A is the amplitude of the perturbation represented by the second term on the RHS, λ_o and ϕ_o set the location of the perturbation, and σ_λ and σ_ϕ the longitudinal and latitudinal extension.

For all simulations we initialize the shallow water model from a state of rest relative to the surface. The model is then allowed to evolve until either a steady state or a periodic state has been reached. We consider that a steady state has been reached if for all fields "a" when $a(x, y, t) = a(x, y, t + t')$ for any t'. We consider that a periodic state has been reached when, for a given period T, $a(x, y, t) \cong a(x, y, t + T)$.

3.3 PV variability on the 370K isentrope

The three upper tropospheric circulation features described in the introduction can also be identified in the upper tropospheric PV field. The westerly jets are associated with bands of sharp meridional PV gradients in the subtropics. The westerly ducts appear as large-scale PV troughs that extend towards the equator. And the equatorial easterly winds may

be seen as regions of relatively low PV to the west of the midlatitude PV troughs (Figure 15a,b and Figure 16a,b).

The different dynamical processes that are associated with each feature are apparent in movies of the PV fields. The propagation of Rossby waves in the subtropical westerly jet appears as a series of propagating synoptic-scale PV troughs and ridges over the mid-latitudes along the jet (Chang and Yu 1999). Rossby wave breaking, which occurs when the PV troughs and ridges propagate over and to the west of the westerly duct, appears as a stretching, thinning, and tilting of the synoptic PV troughs as they lose their coherence (McIntyre and Palmer 1983; Ortega et al. 2016). The advection of eddies over the equatorial easterly winds appears as upper tropospheric PV filaments and eddies, a by-product of the breaking of the synoptic PV troughs, that are advected westward around the PV anticyclone and slowly northward back toward the midlatitudes (Scott and Cammas 2002; Scott et al. 2001).

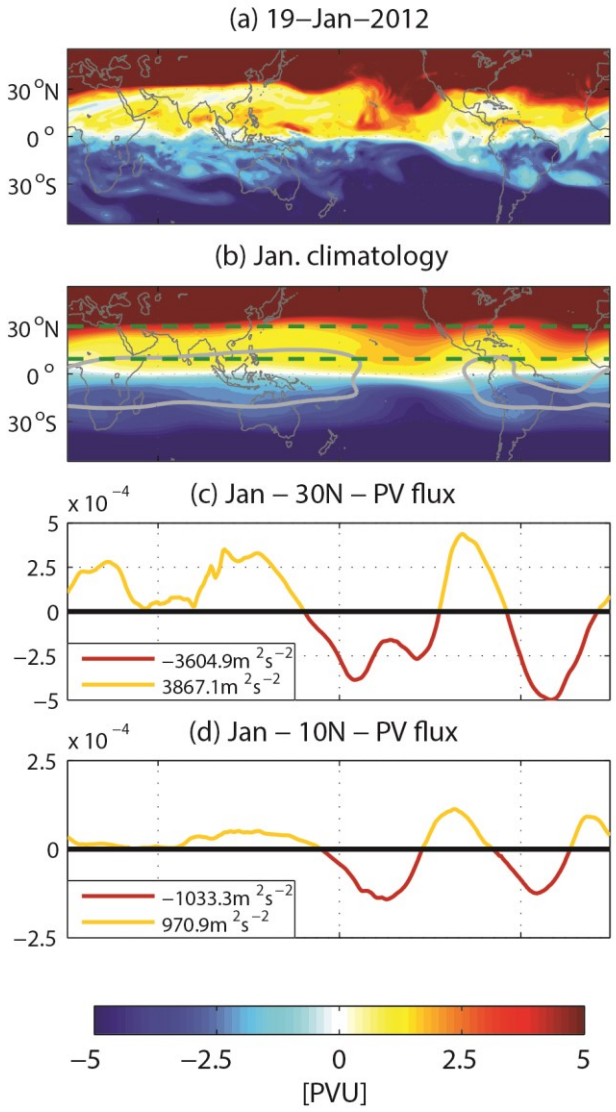

Figure 15 (a) 370K PV field during January 19th, 2012. (b) Climatological 370K PV field for January (shades), boundary between westerlies and easterlies (gray contour), and lines over which PV fluxes are computed (green dashed lines). (c) PV fluxes along 30N (red and yellow curve) and the integrated positive and negative fluxes along such latitude (legend). (d) PV fluxes along 10N and the integrated positive and negative fluxes along such latitude. ERA-interim data.

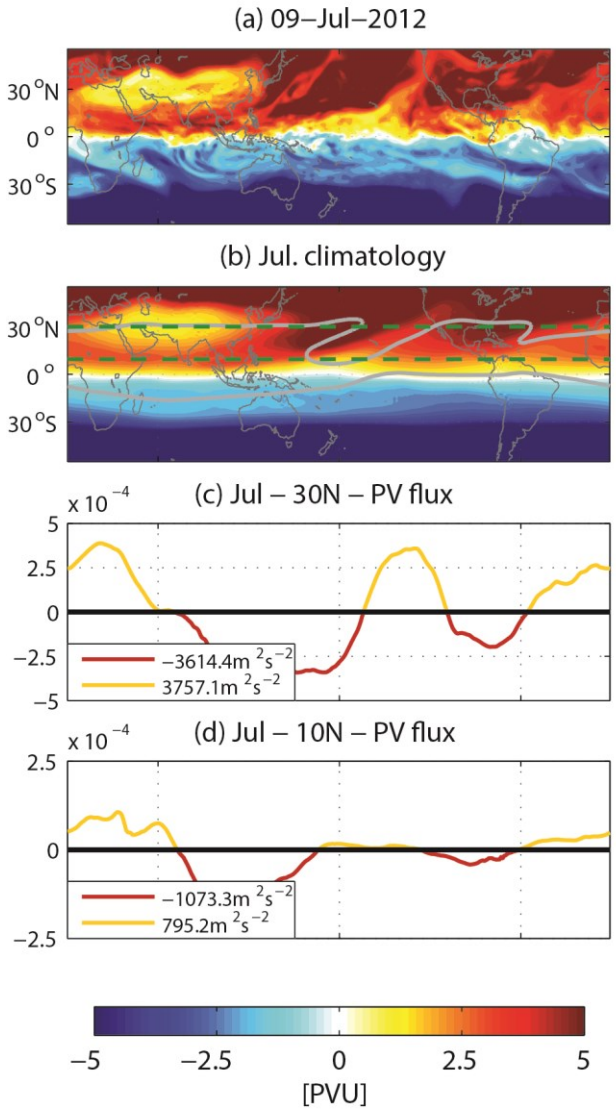

Figure 16 (a) 370K PV field during July 9th, 2012. (b) Climatological 370K PV field for July (shades), boundary between westerlies and easterlies (gray contour), and lines over which PV fluxes are computed (green dashed lines). (c) PV fluxes along 30N (red and yellow curve) and the integrated positive and negative fluxes along such latitude (legend). (d) PV fluxes along 10N and the integrated positive and negative fluxes along such latitude. ERA-interim data.

Figure 15a and Figure 16a suggest that the upper tropospheric features behave in the way that was just described. The figures show the upper tropospheric PV field over Asia and the Pacific Ocean for a representative day during January and July of 2012. They show examples of Rossby waves breaking over, or to the west of, the westerly ducts. During

January (Figure 15a), the PV field over Asia was mostly zonal, and two PV troughs were present over the north Pacific Ocean: the first just west of Japan and the second, over the Pacific Ocean westerly duct, just west of north America. The second PV trough stretched much deeper into the equator than the first, and had some of its PV scattered to its west over the equatorial easterly winds.

During July (Figure 16a), the PV field had a small trough over central Asia and two large troughs over the Pacific Ocean. The PV troughs over the Pacific Ocean had a southwestward tilt, and stretched from the to the Pacific Ocean, west of the westerly ducts, to the Philippines. To the west of the PV troughs, over the Pacific, some of their PV was scattered in a track around the monsoon anticyclone and over the equatorial easterly winds. Further west, over Africa, some of this PV was returning back again to midlatitudes.

As in the study of McIntyre (2008) for the polar vortex, a wave-turbulence "jigsaw picture" emerges for the upper tropospheric tropical atmosphere. There are regions where strong PV gradients prevail and oscillatory motions dominate, and regions where Rossby waves break and their PV is mixed. The former regions are associated with the subtropical westerly jets and the latter are associated with the westerly ducts and the equatorial easterly winds. Yet, perhaps in contrast to the polar vortex, the regions where the breaking occurs more often are quite localized, and are closely related to the location of the westerly ducts (Postel and Hitchman 1999; Scott and Cammas 2002; Waugh and Polvani 2000).

Furthermore, the variability of the upper troposphere is recurrent (in the sense discussed in Christiansen et al. 1997). That is, while the upper tropospheric PV field never returns exactly to a previous configuration, as is expected in turbulent flows, the field display a

quasi-periodic behavior associated with its Rossby wave-dynamics. Throughout the year, Rossby waves repeatedly propagate eastward on the subtropical westerly jet, break within the westerly ducts, and then mix within the equatorial easterly winds and recirculate back to midlatitude as eddies.

The repeated breaking of Rossby waves over the westerly ducts leads to advective fluxes of midlatitude PV towards the tropics. Moreover, divergent circulation over the equatorial easterly winds, and the beta-drift of eddies, leads to advective PV fluxes towards midlatitudes. These fluxes, can be computed on an isentrope as

$$\boldsymbol{J_A} = \sigma q \boldsymbol{v} \tag{8}$$

Where σ is the is the mass density, q the PV, and $\boldsymbol{v} = (u, v, 0)$ the wind vector in isentropic coordinates. Further, the flux through a given latitude circle is given by

$$\boldsymbol{J_A} \cdot \boldsymbol{n} = \sigma q v \tag{9}$$

where $\boldsymbol{n} = (0, -1, 0)$ is a vector that points towards the equator along the latitude circle on the isentrope.

Figure 15c and Figure 16c show climatological advective PV fluxes around 30N°, computed from Equation 9, for January and July. During January, negative PV fluxes (i.e., PV fluxes towards the equator) are observed shifted slightly to the west of the westerly ducts, and positive PV fluxes are observed elsewhere around 30°N. During July, negative PV fluxes are also observed to the west of the westerly ducts, yet further west than before, and positive PV fluxes are again observed elsewhere around 30°N.

Figure 15c and Figure 16c further illustrate an important property: the sum of the positive and negative advective fluxes, for both seasons, is nearly in balance. That is, along 30°N on isentrope 370K

$$\oint_{30°N} \boldsymbol{J_A} \cdot \boldsymbol{n}\, dl \cong 0 \tag{10}$$

where $\boldsymbol{n}$ is a unit vector that point towards the equator everywhere around 30°N and dl is the differential length element. The balance along 30°N is more closely met during July than during January, and in both cases positive fluxes along the latitude circle are dominant. That is, along 30°N the right hand side of Equation 10 adds up to a small positive number both during July and January.

Finally, Figure 15d and Figure 16d show the climatological advective PV fluxes around 10°N for both January and July. The PV fluxes along the 10°N have a smaller amplitude than those along 30°N, are displaced slightly to the west relative to the 30°N fluxes, and have dominant negative fluxes. As before, and in accordance with Equation 10, the positive and negative fluxes seem to be in close balance, although the balance is not as close during July.

3.4 The nature of PV fluxes in between isentropes

The near balance of PV fluxes can be understood through the so-called "impermeability theorem" of the atmosphere (Haynes and McIntyre 1987; Haynes and McIntyre 1990). The theorem describes two fundamental facts about PV fluxes: (i) that there are no sources or

sinks of PV between isentropes that do not intersect the ground, even in the presence of diabatic and frictional processes, and (ii) that a PV flux across isentropes cannot occur.

Consider the equations of PV and mass conservation in isentropic coordinates:

$$\frac{dq}{dt} = \frac{1}{\sigma}\left(\boldsymbol{\eta} \cdot \nabla\dot{\theta}\right) + \frac{1}{\sigma}\boldsymbol{k} \cdot \nabla \times \boldsymbol{F} \tag{11}$$

$$\frac{\partial\sigma}{\partial t} + \nabla_\theta \cdot (\sigma\boldsymbol{v}) + \frac{\partial}{\partial}\left(\sigma\dot{\theta}\right) = 0 \tag{12}$$

Where $\boldsymbol{\eta}$ is the absolute vorticity vector, $\mathbf{F} = \left(F_x, F_y, 0\right)$ represents dissipative processes, θ is the isentropic level, $\boldsymbol{k}$ a unit vector perpendicular to the isentropic level, and $\dot{\theta}$ the diabatic heating term. By multiplying Equation 11 by σ and rearranging the resulting equation using Equation 12, one obtains the impermeability theorem

$$\frac{\partial(\sigma q)}{\partial t} + \nabla \cdot \boldsymbol{J} = 0 \tag{13}$$

where $\boldsymbol{J} = \boldsymbol{J_A} + \boldsymbol{J_{\dot{\theta}}} + \boldsymbol{J_F}$ is the total flux of PV along the isentrope, $\boldsymbol{J_{\dot{\theta}}} = \left(\dot{\theta}\,\partial v/\partial\theta\,, -\dot{\theta}\,\partial u/\partial\theta\,, 0\right)$ is the contribution due to diabatic heating, $\boldsymbol{J_F} = \left(-F_y, F_x, 0\right)$ is the contribution due to frictional terms, and $\boldsymbol{J_A} = \sigma q\boldsymbol{u}$ represents the advective flux of PV. Importantly, none of these fluxes has components across isentropes, they point strictly along the isentropic surfaces. Furthermore, Equation 13 has no source terms, with its right hand side always equating to zero.

Equations 12 and 13 can be further simplified by considering the recursive character of the upper levels. Specifically, we can remove the temporal tendency of the equations by integrating over a long enough period (T). That is, for a given field a, such that $a(x, y, t) \cong a(x, y, t + T)$ we must have

$$\int_{t}^{t+T} \frac{\partial a}{\partial t} dt \approx 0 \tag{14}$$

Carrying this operation for Equations 12 and 13, and assuming that advective fluxes are of first order importance (i.e. $\boldsymbol{J_{\dot{\theta}} \sim J_F \sim 0}$,), we obtain the following two equations

$$\nabla \cdot (\boldsymbol{u}\sigma q) \approx 0 \tag{15}$$

$$\nabla \cdot (\sigma \boldsymbol{V}) \approx S \tag{16}$$

where $S = -\frac{\partial}{\partial \theta}\left(\sigma \dot{\theta}\right)$ is the time rate change of mass in between isentropes induced by their differential change in velocities; that is, a mass source in between the isentropes.

Equations 15 and 16 can be used to understand the close balance of PV fluxes along $30°N$. Consider an atmosphere that is everywhere adiabatic except for the equator and parallels $\pm\phi_{Sink}$ on an isentrope of the upper troposphere (Figure 17; red and blue lines). Assume that S, on such isentrope, can be written as

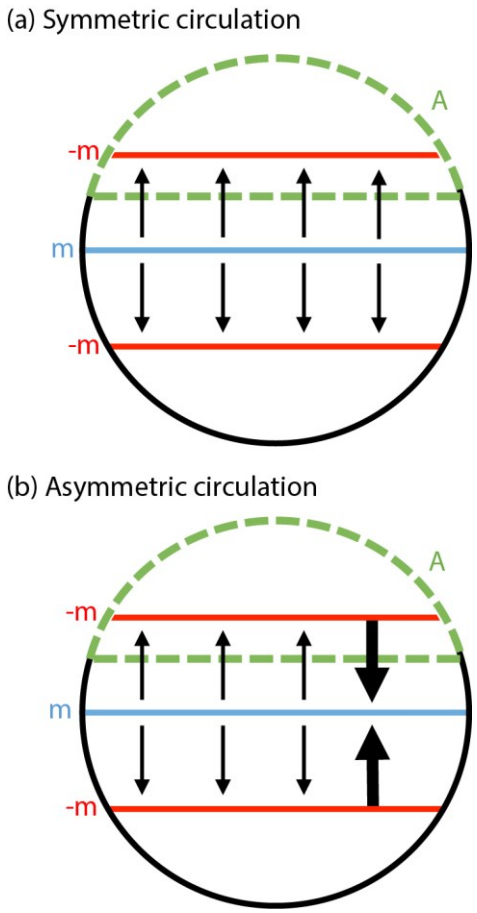

Figure 17 Idealized flow in an upper tropospheric isentrope that surrounds the globe. Blue lines represent mass sources and red lines represent mass sinks. A circulation is expected to develop, going from the mass sources towards the mass sinks. We consider two possibilities: (a) a circulation that goes everywhere poleward and (b) a circulation that goes poleward on a zonally averaged sense. In the absence of dissipation and diabatic processes, a circulation that goes everywhere poleward can only develop if its PV is zero everywhere along the poleward flow (black arrows, top figure), so that the PV flux through a given latitude (green dashed curve) is exactly zero. A circulation that goes poleward on a zonally average sense can develop even if its PV is not zero everywhere. In this case equatorward return fluxes of PV (big black arrows, bottom figure) must develop in response to the poleward PV fluxes, moreover, the different fluxes balance each other.

$$S(\phi) = \frac{m}{2\pi R}\,\delta(\phi - 0) - \frac{m}{4\pi R\,cos\,\phi_{Sink}}\,\delta(\phi + \phi_{Sink}) - \frac{m}{4\pi R\,cos\,\phi_{Sink}}\,\delta(\phi - \phi_{Sink}) \tag{17}$$

where

$$\delta(\phi - x) = \begin{cases} 1 \rightarrow x = \phi \\ 0 \rightarrow x \neq \phi \end{cases} \tag{18}$$

is the Dirac-delta function. Equation 17 then corresponds to a zonally symmetric mass source over the equator with two zonally symmetric sinks over $\pm\phi_{Sink}$ that exactly balance the equatorial source. That is, the global integral of *S* adds up to zero

$$\iint S dA = 0 \tag{19}$$

Now consider a parallel ϕ_o that is between the equator and ϕ_{Sink}. Integrating Equation 16 over the region north of ϕ_o (green dashed curve in Figure 17) shows that the mass fluxes around ϕ_o must balance the sink at ϕ_{Sink}. That is,

$$\iint S dA = \iint \nabla \cdot (\sigma \boldsymbol{v})\, dA = \oint_{\phi_o} (\sigma \boldsymbol{v}) \cdot \boldsymbol{n}\, dl = -\frac{m}{2} \tag{20}$$

Integrating the impermeability theorem (Equation 15) over the same region gives

$$\iint \nabla \cdot (\sigma q \boldsymbol{v})\, dA = \oint_{\phi_o} (\sigma q \boldsymbol{v}) \cdot \boldsymbol{n}\, dl = 2\pi R \cos\phi_o\, [\sigma q v] = 0 \tag{21}$$

where R is Earth's radius, and we have defined the zonal average operator for a field a, along a latitude ϕ, as

$$[a] = \frac{1}{2\pi R \cos\phi} \oint_{\phi} a \, dl \tag{22}$$

Now, if we assume that $\boldsymbol{v}$ has a northward component everywhere (Figure 17a), then, in order for Equation 21 to be satisfied, σq must vanish everywhere along ϕ_o. However, if we relax this assumption, and only assume that the zonal average of $\boldsymbol{v}$ has a northward component, then Equation 21 implies that there must be a southward PV flux somewhere along ϕ_o that balances the northward flow of PV associated with the zonally averaged circulation (Figure 17b).

3.4.1 The effect of the PV fluxes in the upper tropospheric circulation

Equation 15 is only an approximate expression as the advective PV fluxes are never exactly in balance, and both $J_{\dot{\theta}}$ and J_F will usually have finite values. This imbalance of the advective PV fluxes is required to maintain the features of the upper level circulation. To see this, consider the equations of motion written as in (Hsu and Arakawa 1990), which emphasize the role of PV fluxes:

$$\frac{\partial \boldsymbol{v}}{\partial t} = -\sigma q \boldsymbol{k} \times \boldsymbol{v} - \nabla_\theta M - \dot{\theta} \frac{\partial \boldsymbol{v}}{\partial \theta} + \boldsymbol{F} \tag{23}$$

where M is the Montgomery stream function. The zonal component of Equation 23 is simply

$$\frac{\partial u}{\partial t} = -\sigma q v - \frac{\partial M}{\partial x} - \dot{\theta} \frac{\partial u}{\partial \theta} + F_x \tag{24}$$

Taking the zonal average of Equation 24, dropping the temporal derivatives by assuming either a steady state or a recurrent state (Equation 14), and assuming that $F_x = -ku$, where k is a linear damping coefficient, we obtain a relation between the zonally averaged features of the circulation, the zonally averaged PV fluxes, and the momentum fluxes due to diabatic processes. This relation reads

$$[u] \approx \frac{1}{k}\left\{[\sigma q v] + \left[\dot{\theta}\frac{\partial \mathrm{u}}{\partial \theta}\right]\right\} \tag{25}$$

Moreover, in an adiabatic atmosphere

$$[u] \approx \frac{1}{k}\,[\sigma q v] \tag{26}$$

Thus, the imbalance of the advective PV fluxes can have a direct effect on the zonally averaged meridional winds. We assume a linear damping here for illustrative purposes, but similar arguments could be made with other forms of the damping.

3.5 A shallow water model of the upper troposphere

The ideas discussed above can be easily explored in experiments of the shallow water model discussed in Section 3.2. The shallow water model has no representation of the vertical momentum transport of the atmosphere (i.e., $\dot{\theta}\,\partial u/\partial\theta$), yet is a good approach for at least three reasons. First, the equations of motion along isentropes for the real atmosphere are analogous to the equations of motion of the shallow water model. Second, we can choose the dissipative terms of the model to be a linear damping, so that an

analogous equation to Equation 26 applies. Third, the concept of recurrence can be easily exploited as the results of the model turn out to be almost exactly periodic.

The curl of the shallow water momentum equation (Equation 4) produces the shallow water version of the impermeability theorem[10]:

$$\frac{\partial hq}{\partial t} + \nabla \cdot (\boldsymbol{u}hq + \boldsymbol{F}) = 0 \tag{27}$$

where $\boldsymbol{F} = -k\boldsymbol{u}$, and k is a linear damping coefficient. If advective PV fluxes are dominant, then

$$\frac{\partial hq}{\partial t} + \nabla \cdot (\boldsymbol{u}hq) \cong 0 \tag{28}$$

Further, if the shallow model results are exactly periodic. That is, if $a(x, y, t) = a(x, y, t + T)$ for a given field a and a period T, then

$$\int_t^{t+T} \frac{\partial a}{\partial t} dt = 0 \tag{29}$$

[10] Alternatively, and more illuminating, one could follow an analogous procedure to that used in deriving Eq. 13. That is, by multiplying Eq. 4 by h and using Eq. 5 to obtain Eq. 27. However, the procedure followed in the main text has the advantage of showing that the impermeability theorem is a version of the equation of absolute vorticity that emphasizes PV fluxes.

which is an exact version of Equation 14. The PV flux and mass conservation equations then simplify to

$$\nabla \cdot (\boldsymbol{u}hq) \cong 0 \tag{30}$$

$$\nabla \cdot (h\boldsymbol{V}) = S \tag{31}$$

By analogous arguments to that of Equation 15 to 21, these last two equations imply that there cannot be a circulation that goes everywhere poleward in the shallow water model, unless $hq = 0$, and that alternating positive and negative PV fluxes along latitude circles should be expected when advective terms are dominant.

Moreover, the effect of PV fluxes on the shallow water model is analogous to that in between isentropes of an adiabatic atmosphere (Equation 26). Consider, the zonal component of Equation 4

$$\frac{\partial u}{\partial t} - qhv = -\frac{\partial}{\partial x}(K_E + gh) - ku \tag{32}$$

Integrating over a period (Equation 29), or in steady state, we obtain

$$-qhv = -\frac{\partial}{\partial x}(K_E + gh) - ku \tag{33}$$

and taking the zonal average gives

$$[u] = \frac{1}{k}[qhv] \tag{34}$$

Equation 34 is exact when the results from the shallow water model are either periodic or steady. Thus, in such cases there is a clear relation between the PV fluxes and the circulation features of the shallow water model.

3.5.1 Results for two modelling experiments

We present results of two experiments conducted with the shallow water model. The first experiment, which we refer to as the maritime experiment, is intended to represent the effect that deep convection over the maritime continent has on the tropical upper troposphere. The second experiment, which we refer to as the monsoon experiment, is intended to represent the effect that deep convection over South Asia and the sensible heating of the Tibetan Plateau have on the upper troposphere circulation.

For the maritime continent experiment, we force the shallow water model using an equilibrium height (h_e) that peaks over the equator. Specifically, we set $\lambda_o = 0$, $\phi_o = 0$, $A = 30000m$, $\sigma_\phi = 6°, \sigma_\lambda = 10°$, and $\tau = \frac{1}{10} day^{-1}$ in Equation 7. We include the mass forcing S from the first time step, and leave it on for the rest of the simulation. A steady state is reached after the initial transients of the model dissipate.

For the monsoon experiment we force the shallow water model using an equilibrium height (h_e) that peaks over 30°N. We set $\lambda_o = 0$, $\phi_o = 30°$, $A = 30000m$, $\sigma_\phi = 6°$, $\sigma_\lambda = 10°$, and $\tau = \frac{1}{10} day^{-1}$. As before, we include the mass forcing S from the first time step, and leave it on for the rest of the simulation. A periodic, or closely periodic, solution is reached after the initial transients of the model dissipate.

Different stages of the periodic solution of the monsoon experiment are shown in Figure 18. While the simulation turns out to be almost exactly periodic, it also displays characteristics that are often associated with geophysical-turbulence. The PV field is constantly pulled from midlatitudes, forming a PV trough to the east of the forcing. This trough gets thinner as it is pulled towards the equator, it folds onto itself, and then detaches from the main trough as and eddy. The whole process is then one that facilitates the mixing (in the sense discussed in Cvitanović et al. 2012) of PV over the equatorial region, allowing for dissipative terms to act more efficiently.

Figure 19a shows the steady state PV field for the maritime continent experiment and Figure 20a shows the time averaged PV field of the monsoon experiment. As for the upper tropospheric circulation, both experiments have subtropical westerly jets that are associated with sharp PV gradients over the midlatitudes, westerly ducts that are associated with midlatitude PV troughs that extend towards the equator, and equatorial easterly winds that are to the west of these midlatitude PV troughs.

However, there are important differences between the experiments and the observed upper tropospheric circulation. For the maritime continent experiments the equatorial easterly winds extend over a much smaller region than in the real atmosphere and, correspondingly, the westerly ducts extend over a much larger region. For the monsoon experiments, the equatorial easterly winds completely surround the equator and tend to have a much more zonal structure than in the real atmosphere. The monsoon experiment westerly ducts are observed as small intrusions of westerly winds into the equatorial easterlies. To the south of the westerly ducts the speeds the equatorial easterly winds decreases considerably.

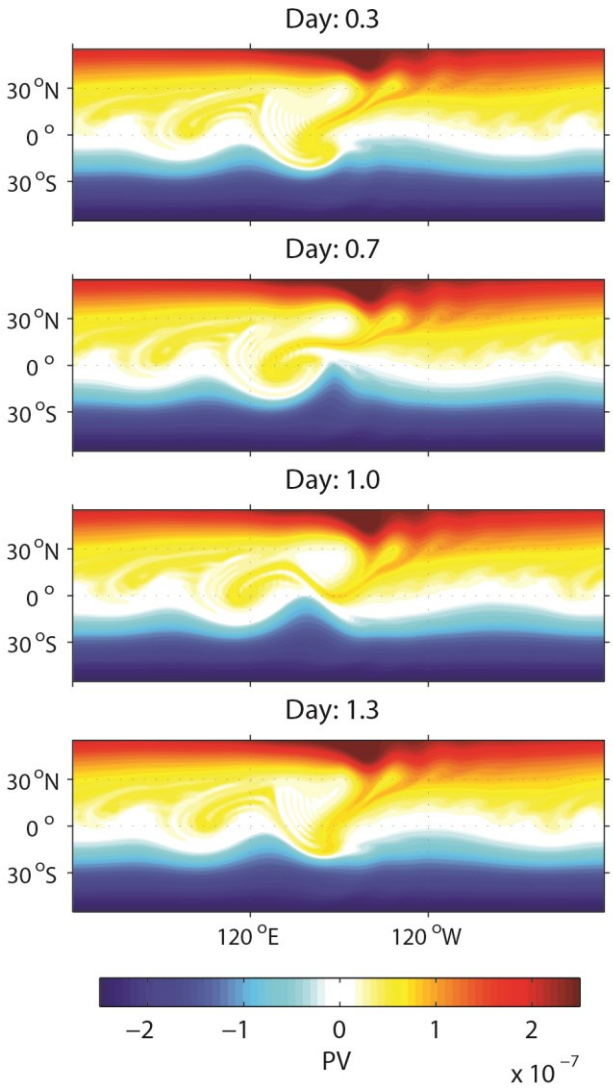

Figure 18 Periodic solution of the shallow water monsoon experiment. The potential vorticity field is show. Notice how the PV field is stretched, folded, and mixed.

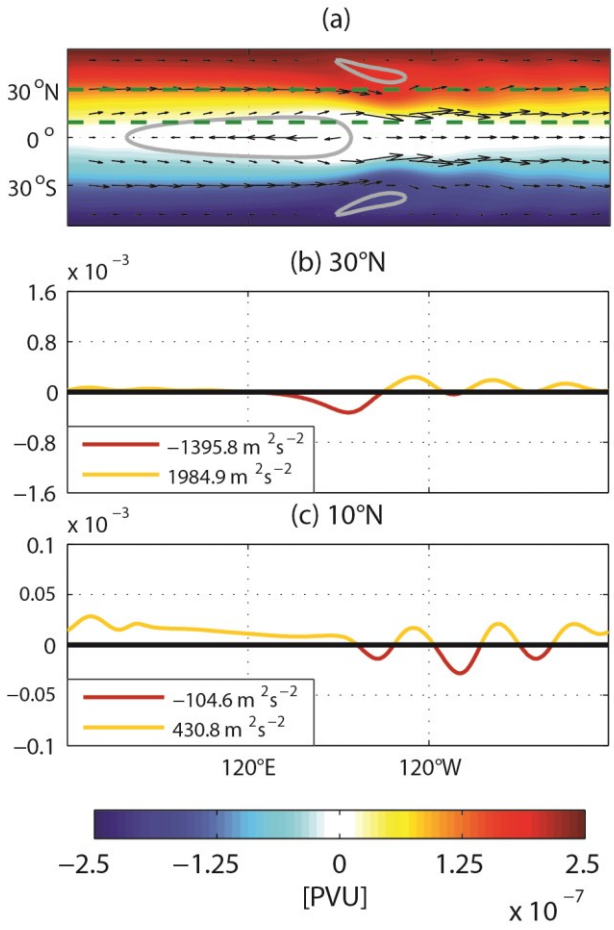

Figure 19 (a) Steady state PV field of the shallow water maritime continent experiments (shades) and its steady state winds (black arrows). (b) PV fluxes along 30N (red and yellow curve) and the integrated positive and negative fluxes along such latitude (legend). (c) PV fluxes along 10N and the integrated positive and negative fluxes along such latitude.

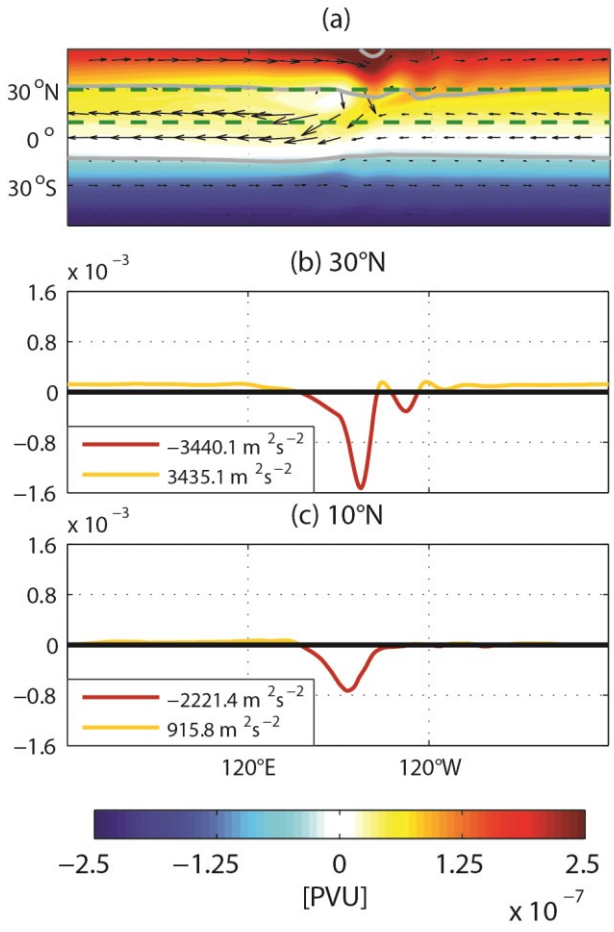

Figure 20 (a) Time averaged PV field of the shallow water maritime continent experiments (shades) and its time averaged winds (black arrows). (b) Time averaged PV fluxes along 30N (red and yellow curve) and the integrated positive and negative fluxes along such latitude (legend). (c) Time averaged PV fluxes along 10N and the integrated positive and negative fluxes along such latitude.

Figure 19b and Figure 20b show the advective PV fluxes computed along 30°N for the shallow water experiments. As for the upper troposphere, PV fluxes towards the equator are shifted slightly to the west of the westerly ducts, and poleward PV fluxes occur elsewhere. The advective fluxes are dominant along 30°N in both experiments, but they do not balance as closely for the maritime continent experiments as they do for the monsoon experiment. Figure 19c and Figure 20c show the advective PV fluxes computed along

10°N. The advective fluxes computed along this parallel do not balance closely for any of the two experiments, and the greatest imbalance is seen for the monsoon experiment.

Finally, Figure 21 shows the right and left side of Equation 34, for both experiments, as two different curves that are a function of latitude. The red dashed curves correspond to the steady state, or temporally mean state, of the zonally averaged meridional PV fluxes divided by the dissipation coefficient (i.e., $[hqv]/k$). The black curves correspond to the steady state, or temporally averaged state, of the zonally averaged zonal winds (i.e., $[u]$). In both experiments, an in accordance with Equation 34, both curves closely follow each other. The equatorial easterly winds are associated with negative zonal averages of the PV fluxes, and the subtropical westerly jet is associated with positive zonal averages of the PV fluxes. For the monsoons experiments, where the periodic solution is obtained, Figure 21b also shows that there is a large variation of the zonally averaged PV fluxes (light-blue curves), whose temporal average results in the zonally averaged winds.

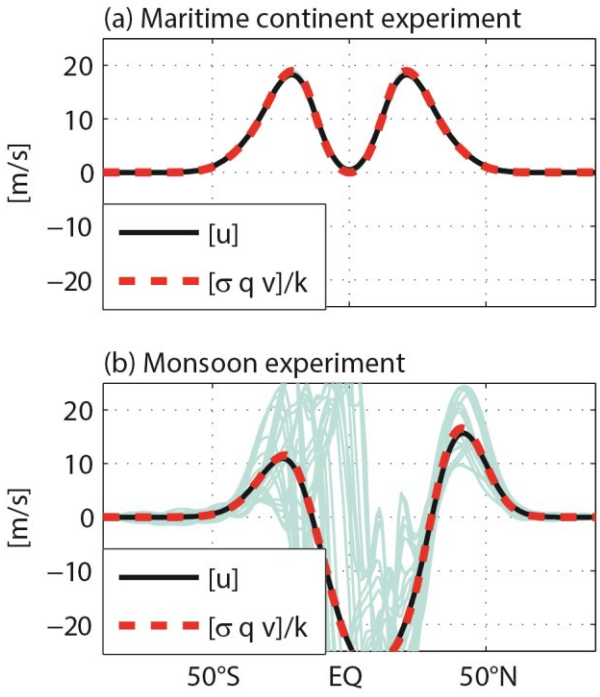

Figure 21 (a) Steady state zonally averaged zonal winds (black curve) and the zonally averaged PV fluxes for the maritime continent experiments (red dashed curve). (b) Temporally and zonally averaged zonal winds (black curve), temporally and zonally averaged PV fluxes (red dashed curve), and the instantaneous zonally averaged PV fluxes for different time steps of the simulation (light-blue curve). In all cases the PV fluxes were divided by the dissipation coefficient.

3.6 Discussion

We studied the upper level circulation of the tropical atmosphere. We defined three main features of the circulation (the subtropical westerly jets, the westerly ducts, and the equatorial westerly winds), and discussed how they interact via Rossby wave-dynamics: Rossby waves travel on the subtropical westerly jet, break over the westerly ducts, and are then advected westward, and slowly northward, as eddies over the equatorial easterly winds. We suggested that this variability is recurrent, the same cycle repeating with slight

variations, and show that it leads to alternating PV fluxes, towards and away from the equator, that closely balance each other around latitude circles.

By considering the atmospheric impermeability theorem (Equation 13) we showed that a close balance of the advective fluxes is to be expected when dissipative and diabatic fluxes are small. We showed that such balance implies that an upper tropospheric circulation that is everywhere poleward is unlikely to develop. That is, that unless $\sigma q = 0$ everywhere in the poleward branch of the circulation, fluxes of PV towards the equator would have to eventually develop. Moreover, we suggested that the imbalance of the advective PV fluxes, the dissipative and diabatic PV fluxes, maintain the mean winds of the atmosphere (Equation 25).

We studied the results of two shallow water experiments to test our ideas. We designed the experiments to represent the circulation of the upper atmospheric levels during January and July. The first of these experiments, the maritime continent experiment, evolved into a steady state and displayed weak easterlies. The second of the experiments, the monsoon experiment, evolved into a periodic state and displayed strong easterlies that surrounded the equator. The relation between the different features of the shallow water experiments and their PV field was similar to that of the real atmosphere, although important differences were also observed.

The balance implied by Equation 30 was more closely met in the monsoon experiment close to 30°N, where the zonally average winds were near zero (as it is expected from Equation 34). However, around 10°N of the monsoon experiment, and around both 10°N and 30°N of the maritime continent experiment, there was a strong imbalance between the

northward and southward PV fluxes; consistent with the winds that developed around these latitudes. The strong imbalance of the monsoon experiment around 10°N was most likely due to the "turbulent" nature of the simulation, which allowed for dissipative processes to act more efficiently. The strong imbalance of the maritime continent experiments was also likely due to dissipative processes.

Finally, Equation 34 was closely met in both experiments, plots of the zonal averages of u and of hqv/k were almost indistinguishable (Figure 21). This shows that PV fluxes in the shallow water model maintain its zonally averaged mean circulation, and suggest a similar role for PV fluxes in the real atmosphere.

3.6.1 On the recurrent motions of the shallow water experiments and the atmosphere

The periodic behavior of the shallow water experiments and the recurrent behavior of the upper tropospheric PV fields lead to simplified forms of the impermeability and mass continuity equations when integrated over a long enough period (Equations 15,16 and 30,31). For the shallow water experiments, which were either steady or periodic, the period is the time it takes the PV field to exactly recur.

The simplified forms of the impermeability and mass continuity equations points to a balance between the mass sources in between isentropes (due to deep convection) and the planetary-scale dynamics of the atmosphere. This balance seems achieved via Rossby-wave dynamics: divergent circulations induced by the mass sources constantly displace PV towards midlatitudes, and the PV field responds by constantly radiating Rossby waves through the subtropical westerly jets, which then break within the westerly ducts, and are then advected as eddies over the equatorial easterly winds. The role of Rossby-wave

dynamics in maintaining such balance is then analogous to that of Lighthill radiation in the context of maintaining geostrophic balance (McIntyre 2001), where gravity waves are constantly radiated to achieve geostrophic balance. Here, however, Rossby waves are the ones being constantly radiated, and the "balance" might not be a steady but a recurring and turbulent state of the upper troposphere.

3.6.2 A note on the implications for mid-tropospheric circulations

In this study we emphasized the circulation on the 370K isentrope. This is a convenient level to study as it never intersects the ground, and because dissipative processes tend to be small on the upper troposphere, where the isentrope resides. However, there are lower isentropes that display similar behavior.

Figure 22 shows the climatological 330K PV field for the month of January. Isentrope 330K does not intersect the ground during this time and is close to the 500mb level during January. The PV field has many similarities with the 370K PV field of January, a sharp gradient associated with the subtropical westerly jet, a large-scale PV trough over the westerly ducts, and relatively low PV values to the west of this through, extending from the west Pacific Ocean to the Indian Ocean, where the Madden-Julian Oscillation often develops (Madden and Julian 1972; Zhang and Ling 2011).

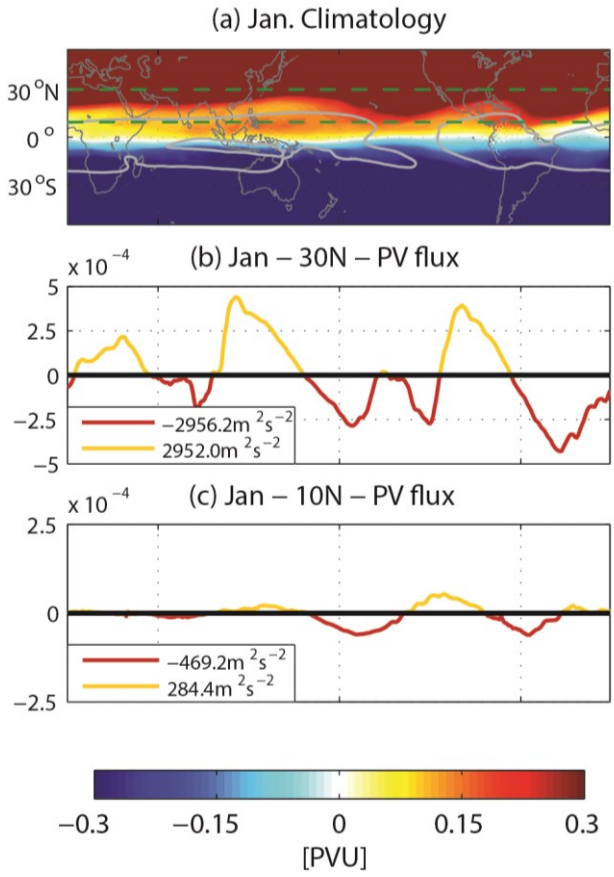

Figure 22 (a) Climatological 330K PV field for January (shades), boundary between westerlies and easterlies (gray contour), and lines over which PV fluxes are computed (green dashed lines). (b) PV fluxes along 30N (red and yellow curve) and the integrated positive and negative fluxes along such latitudes (legend). (c) PV fluxes along 10N and the integrated positive and negative fluxes along such latitudes. ERA-interim data.

3.6.3 A note on the study of recurrent motions in dynamical systems

The periodic character of the shallow water monsoon experiments suggests a clear relationship between its PV fluxes and its circulation. It allowed us to link the effect of Rossby wave dynamics to the maintenance of the mean features of its circulation. Yet, the periodic character of the experiment might not be essential to study such links, for a recurrent experiment (i.e., a quasi-periodic one) similar theories might apply.

Dynamical systems, such as the shallow water system, often remain close to invariants of their dynamics. Such invariants are solutions of the dynamical system that have either exactly periodic or steady behavior. For instance, the dynamics of the shallow water experiments is such that it remains close to the steady state solution implied by Equations 30 and 31 (Figure 20a and Figure 21a). Moreover, the close periodicity of the monsoon experiments (Figure 18) suggests that the solution stays close to a periodic orbit. In generic dynamical systems, however, the invariants of the dynamics are usually unstable and give rise to recurrent behaviors. This makes it difficult to find these invariants, but different techniques have been developed for this. Moreover, once the invariants are found, statistical features of the dynamical system can be evaluated (Cvitanović 2013; Cvitanović et al. 2012). Finding these invariants might then help to understand the role that recurrent structures, such as those due to Rossby wave dynamics, can have on the large-scale atmospheric circulation.

3.7 Acknowledgements

The Climate Dynamics Division of the National Science Foundation, under Grant NSF-AGS 0965610, provided funding support for this research.

CHAPTER 4. DISCUSSION

The results of this work suggest that the tropics and midlatitudes are closely linked. Their link is dynamical, arising due to the tendency of the atmosphere to conserve its angular momentum, and it is most easily described by studying the PV field of the upper troposphere. On such field, midlatitude Rossby waves are seen to repeatedly propagate eastward on the subtropical westerly jet, break within the westerly ducts, and then mix, and recirculate back to midlatitudes, within the tropical easterly winds. The spatial characteristics of the PV field, and the upper tropospheric circulation, can be best described by dividing the tropics into features over which different dynamics occur (McIntyre 2008; Webster and Chang 1988; Webster and Holton 1982), while their temporal evolution can be best described by exploiting their recurrence (Christiansen et al. 1997; Cvitanović et al. 2012).

The results of this work also suggest a link between the intraseasonal variability of the lower and upper tropical troposphere. The results show that the upper tropospheric UQBW, which is related with the lifecycle of the Rossby waves just described, might have an effect on the lower tropospheric QBW. In a composite analysis of the UQBW, Rossby waves along the subtropical westerly jet were observed both before, and after, observing a convective phase of the lower tropospheric QBW. Thus, better predictability of tropical weather systems might be obtained through a better monitoring and modelling of the UQBW.

As a first approximation, the variability of the upper tropospheric PV field can be thought of as the result of the mean divergent circulation set up by deep convection in the tropical upper troposphere. This divergence pushes PV towards the poles and triggers midlatitude Rossby waves. The waves propagate eastward, away from the region of deep convection, and generate PV fluxes towards the tropics when they break over the westerly ducts. These fluxes towards the tropics compensate PV fluxes towards the poles that were generated by deep convection and, therefore, keep the global PV in balance. Thus, in keeping the global PV in balance, Rossby waves play a role analogous to that of gravity waves when a vortex is kept close to geostrophic balance, or to acoustic waves when a flow is kept close to being incompressible.

We now briefly summarize the main contributions of this work, and then discuss important questions that have emerged from it. The following were the main contributions and conclusions of Chapter 2:

- We characterized the UQBW of the South Asian monsoon in terms of the 370K PV field and showed that the UQBW is a recurrent boreal summer phenomenon that follows a typical sequence of events and that involves interactions between the midlatitudes and the tropics.
- We showed that there is a correlation between the UQBW and the lower tropospheric QBW of the South Asian monsoon.
- We presented the case study of tropical typhoon Fengshen, for which the interaction between the lower and upper troposphere was likely to be important.

- We emphasized the importance of studying the UQBW. We showed that its variability seems to be coupled to the QBW and discussed possible implications for weather forecasting in the region.

The main contributions and conclusions of Chapter 3 were:

- We defined three main features of the upper tropospheric circulation (the subtropical westerly jets, the westerly ducts, and the equatorial westerly winds), and discussed how they interact via Rossby wave-dynamics.
- We showed that a close balance of the advective PV fluxes in the upper troposphere implies that an upper tropospheric circulation that is everywhere poleward is unlikely to develop. This suggest that assumptions of zonally symmetry are inadequate to model the planetary scale circulation of the tropical atmosphere, and makes of westerly ducts an integral response of the upper tropospheric circulation. Moreover, it implies that phenomena such as the UQBW should always be expected.
- We suggested that the imbalance of the advective PV fluxes helps maintain the mean winds of the upper troposphere. Moreover, we showed how this is exactly the case for a shallow water model of the atmosphere.
- We suggested that the role of Rossby waves is to maintain a global balance of PV, and suggested that this role is analogous to that of acoustic waves maintaining fluids close to being incompressible, or to gravity waves maintaining geostrophic balance.

- We emphasized the importance of considering the recurrent motions of the atmosphere in under to understand its dynamics, and showed how this could be used in the case of periodic simulation of a shallow water model.

Several important question remain unanswered in this work, and will hopefully lead to further research. For instance, there is the question regarding the possible connection between the UQBW and the QBW. It is important to determine if the UQBW can affect the QBW, as this would have implication both for weather forecasting and for the way we understand the coupling between the upper and lower troposphere.

At the moment, however, the possibility that the UQBW might affect the QBW is often disregarded by arguing that balance dynamic scalings do not allow for a thin upper tropospheric anomaly, such as the UQBW, to affect the lower tropospheric levels over the tropics. Yet, if this is the case, why do we see a subtropical Rossby wave on the UQBW composites several days before a convective phase of the QBW?

In the forecasting of tropical cyclones, the importance of the upper tropospheric levels is heavily emphasized. Upper tropospheric troughs, that seem related with the UQBW, are known to aid the formation of tropical cyclones by facilitating upper level divergence and reducing the wind shear for these systems (Sadler, 1976). Thus, a connection between the UQBW and the QBW should not be disregarded just yet.

Their connection, or lack thereof, could be tested by means of an atmospheric model that is shown to reproduce the variability of the UQBW and the QBW and that has the ability to include different convective parametrizations schemes. By testing these parametrizations and evaluating the implication these have for the coevolution between the

UQBW and the QBW, one could conclude whether the two oscillations are indeed coupled. This approach was used in the study of Slingo (1998) to test the relation between upper tropospheric troughs and deep convection over the Pacific Ocean.

Moreover, the physics behind the UQBW might be out of the realm where balance dynamics applies. The UQBW is in part the result of breaking Rossby waves, so its associated PV is extensively stretched and mixed. Is it possible that this strong mixing triggers particularly strong gravity waves that are not accounted for with balance dynamics?

APPENDIX A. GENERAL CONCEPTS REGARDING THE PV FIELD

PV is a dynamical quantity. It is a measure of the vorticity of fluid parcels weighted by their vertical stability. The concept was first discussed by Rossby (1936) and was latter put into general mathematical grounds by Ertel (1942; Samelson 2003; Schubert et al. 2004). For the atmosphere, PV is defined as follows:

$$q = \frac{1}{\rho}\boldsymbol{\omega} \cdot \nabla\theta \tag{35}$$

where q is the PV of the atmosphere, ρ its density, $\boldsymbol{\omega}$ its absolute vorticity vector, and θ its potential temperature.

The evolution of the atmospheric PV follows from the equations of motion, and it is given by:

$$\frac{dq}{dt} = \frac{1}{\rho}\boldsymbol{\omega} \cdot \nabla\dot{\theta} + \frac{1}{\rho}\nabla\theta \cdot (\nabla \times \boldsymbol{F}) \tag{36}$$

where $\dot{\theta}$ is the diabatic heating rate and $\boldsymbol{F}$ represents frictional processes (Holton 1992; Hoskins et al. 1985; Nielsen‐Gammon 2012; Vallis 2006). Equation 2 states that PV is conserved under adiabatic and frictionless processes (i.e., $dq/dt = 0$), a fact that allow us to identify midlatitude parcels intruding into the tropical upper troposphere.

Knowledge of the PV field can be used to retrieve of all other atmospheric fields. This retrieval is done in a process known as PV inversion (Davis 1992; McIntyre and Norton

2000) that works remarkably well when balanced dynamics (McIntyre 2003a), such as geostrophic balance, is a good approximation of the dynamics of interest. It works, due to the fact that gravity waves act on the atmosphere comparatively faster than the synoptic motions that determine the weather.

Oscillations of the atmospheric PV field such as propagating ridges and troughs are associated with Rossby waves. These waves are the result of the tendency for PV to be conserved, of the long range effect that a PV anomaly can have on its surroundings, as PV inversion implies, and of the existence of a meridional PV gradient. This last, is the result of earth's geometry.

The simplest PV field that can support a Rossby wave is that which can be represented by two regions of constant PV, one of relatively high PV to the north, and one of relatively low PV to the south. In such case, the contour that divides both regions is of prime importance, because by using PV inversion all the relevant information of the dynamics can be retrieved from a knowledge of the contour's shape. In fact, important numerical methods are based solely on tracking such contours (Waugh and Plumb 1994).

A perturbation of the PV contour, on the simple PV field just described, causes a Rossby wave. Imagine the perturbation as a northward bump in such contour that pushes relatively low PV into the region where high PV use to be (i.e., a ridge). In the real atmosphere, this perturbation could be the result, for instance, of deep convection, which leads to divergent circulations in the upper troposphere (Hoskins and Wang 2006) and therefore pushes PV towards the poles. The perturbation of the contour leads, via PV inversion, to a meridional wind field displaced westward by a quarter wave-length relative to the perturbed contour

(Holton 1992; McIntyre 2008). The wind field then tends to continuously move the perturbation towards the west, relative to the mean flow, and in doing so creates a Rossby wave.

The concept of Rossby-wave breaking follows from the situation discussed above. If the circulation induced by the PV contour leads not to a linear propagation of the Rossby wave (i.e., reversible undulations of the contour) but rather leads to an irreversible displacement of the PV contour, then the Rossby wave is said to break (McIntyre and Palmer 1983). This process of Rossby wave breaking is important for the tropical atmosphere, for instance, in transporting ozone into the tropical upper troposphere (Randel and Park 2006). Moreover, as it is shown in Chapter 3, it is also important for maintaining the mean upper tropospheric winds.

Finally, it should be noted that PV and angular momentum are closely related concepts (DeCaria 2008); studying one is almost equivalent to studying the other. The main difference is, perhaps, the inability of PV inversion to capture Kelvin waves (Schubert and Masarik 2006). Yet, there is no reason to expect that PV will be a concept only useful to study extra-tropical circulations. It should also be useful for the tropics; as conservation of angular momentum is clearly important in both regions. The mere existence of equatorial Rossby and Kelvin waves, and its unequivocal effect in the circulation, is proof of the

importance of PV dynamics on the tropical atmosphere, as both Rossby and Kelvin waves require a PV gradient to develop[11].

[11]Equatorial Kelvin waves need a PV field that has a meridional gradient and changes sign in the domain, that is, and equatorial wave guide. Note that the fact that PV inversion does not capture Kelvin waves is a different matter.

REFERENCES

Annamalai H, Slingo JM (2001) Active/break cycles: diagnosis of the intraseasonal variability of the Asian Summer Monsoon. Climate Dynamics 18:85-102

Arakawa A, Lamb VR (1981) A Potential Enstrophy and Energy Conserving Scheme for the Shallow Water Equations Monthly Weather Review 109:18-36

Chang EK, Yu DB (1999) Characteristics of wave packets in the upper troposphere. Part I: Northern Hemisphere winter Journal of the atmospheric sciences 56:1708-1728

Charney JG (1963) A note on large-scale motions in the tropics Journal of the Atmospheric Sciences 20:607-609

Chatterjee P, Goswami BN (2004) Structure, genesis and scale selection of the tropical quasi-biweekly mode. Quarterly Journal of the Royal Meteorological Society 130(599):1171-1194

Chen T-C, Chen J-M (1993) The 10–20-Day Mode of the 1979 Indian Monsoon: Its Relation with the Time Variation of Monsoon Rainfall. Monthly Weather Review 121:2465-2482

Christiansen F, Cvitanovic P, Putkaradze V (1997) Spatiotemporal chaos in terms of unstable recurrent patterns Nonlinearity 10:55

Cvitanović P (2013) Recurrent flows: the clockwork behind turbulence Journal of Fluid Mechanics 726:1-4

Cvitanović P, Artuso R, Mainieri R, Tanner G, Vattay G (2012) Chaos: Classical and Quantum. Niels Bohr Institute, Copenhagen 2012

Davis CA (1992) Piecewise Potential Vorticity Inversion. Journal of the Atmospheric Sciences 49(16):1397-1411

DeCaria AJ (2008) The Vorticity Equation and Conservation of Angular Momentum Millersville University, http://snowball.millersville.edu/~adecaria/DERIVATIONS/Vorticity.pdf

Dee DP et al. (2011) The ERA-Interim reanalysis: configuration and performance of the data assimilation system Quarterly Journal of the Royal Meteorological Society 137:553-597

Duchon CE (1979) Lanczos Filtering in One and Two Dimensions. Journal of Applied Meteorology 18:1016-1022

Emanuel KA, David Neelin J, Bretherton CS (1994) On large-scale circulations in convecting atmospheres Quarterly Journal of the Royal Meteorological Society 120:1111-1143

Ertel H (1942) Ein neuer hydrodynamischer Erhaltungssatz Naturwissenschaften 30:543-544

Fasullo J, Webster PJ (2003) A Hydrological Definition of Indian Monsoon Onset and Withdrawal. Journal of Climate 16:3200-3211

Fueglistaler S, Dessler AE, Dunkerton TJ, Folkins I, Fu Q, Mote PW (2009) Tropical tropopause layer. Reviews of Geophysics 47

Funatsu BM, Waugh DW (2008) Connections between Potential Vorticity Intrusions and Convection in the Eastern Tropical Pacific. Journal of the Atmospheric Sciences 65:987-1002

Gill AE (1980) Some simple solutions for heat-induced tropical circulation Quarterly Journal of the Royal Meteorological Society 106:447-462

Goswami BN (2012) South Asian monsoon. In: Lau WK-M, Waliser DE (ed) Intraseasonal Variability in the Atmosphere-Ocean Climate System. Springer Berlin Heidelberg

Goswami P, Mathew V (1994) A Mechanism of Scale Selection in Tropical Circulation at Observed Intraseasonal Frequencies. Journal of the Atmospheric Sciences 51:3155-3166

Goswami, B. N. (2003) Clustering of synoptic activity by Indian summer monsoon intraseasonal oscillations. Geophysical Research Letters 30

Gutro R (2008) Hurricane Season 2008: Typhoon Fengshen (Northwestern Pacific Ocean). NASA's Goddard Space Flight Center. http://www.nasa.gov/mission_pages/hurricanes/archives/2008/h2008_fengshen.html

Hack JJ, Jakob R (1992) Description of a global shallow water model based on the spectral transform method. National Center for Atmospheric Research,

Hadley G (1735) Concerning the cause of the general trade-winds: By Geo. Hadley, Esq; FRS Philosophical Transactions 39:58-62

Haynes PH, McIntyre ME (1987) On the Evolution of Vorticity and Potential Vorticity in the Presence of Diabatic Heating and Frictional or Other Forces Journal of the Atmospheric Sciences 44:828-841

Haynes PH, McIntyre ME (1990) On the Conservation and Impermeability Theorems for Potential Vorticity Journal of the Atmospheric Sciences 47:2021-2031

Held IM, Hou AY (1980) Nonlinear Axially Symmetric Circulations in a Nearly Inviscid Atmosphere Journal of the Atmospheric Sciences 37:515-533

Holton JR (1992) An Introduction to Dynamic Meteorology. Academic Press,

Hoskins B (2015) Potential vorticity and the PV perspective Advances in Atmospheric Sciences 32:2-9

Hoskins B, Wang B (2006) Large-scale atmospheric dynamics. In: Wang B (ed) The Asian Monsoon. Springer Berlin Heidelberg

Hoskins BJ (1991) Towards a PV-θ view of the general circulation. Tellus A 43:27-35

Hoskins BJ, McIntyre ME, Robertson AW (1985) On the use and significance of isentropic potential vorticity maps Quarterly Journal of the Royal Meteorological Society 111:877-946

Hoskins BJ, McIntyre ME, Robertson AW (1985) On the use and significance of isentropic potential vorticity maps. Quarterly Journal of the Royal Meteorological Society 111:877-946. Corrigendum 113:402-404

Hoskins BJ, Rodwell MJ (1995) A Model of the Asian Summer Monsoon. Part I: The Global Scale. Journal of the Atmospheric Sciences 52:1329-1340

Hoyos CD, Webster PJ (2007) The Role of Intraseasonal Variability in the Nature of Asian Monsoon Precipitation. Journal of Climate 20:4402-4424

Hsu CJ, Plumb RA (2000) Nonaxisymmetric Thermally Driven Circulations and Upper-Tropospheric Monsoon Dynamics. Journal of the Atmospheric Sciences 57:1255-1276

Hsu Y-JG, Arakawa A (1990) Numerical modeling of the atmosphere with an isentropic vertical coordinate Monthly Weather Review 118:1933-1959

Hurley JV, Boos WR (2014) A global climatology of monsoon low-pressure systems. Quarterly Journal of the Royal Meteorological Society 141:1049-1064

Kikuchi K, Wang B (2009) Global Perspective of the Quasi-Biweekly Oscillation*. Journal of Climate 22:1340-1359

Kiladis GN, Weickmann KM (1992) Extratropical forcing of tropical Pacific convection during northern winter. Monthly Weather Review 120:1924-1939

Knippertz P (2007) Tropical–extratropical interactions related to upper-level troughs at low latitudes. Dynamics of Atmospheres and Oceans 43:36-62

Koteswaram P (1958) The easterly jet stream in the tropics Tellus 10:43-57

Koteswaram P, George CA (1958) On the Formation of Monsoon Depression on the Bay of Bengal Indian Journal of Meteorology & Geophysics 9:9-22

Krishnamurthy V, Ajayamohan RS (2010) Composite Structure of Monsoon Low Pressure Systems and Its Relation to Indian Rainfall. Journal of Climate 23:4285-4305

Krishnamurti TN (1961) The subtropical jet stream of winter Journal of Meteorology 18:172-191

Krishnamurti TN, Ardanuy P (1980) The 10 to 20-day westward propagating mode and "Breaks in the Monsoons". Tellus 32:15-26

Krishnamurti TN, Bhalme HN (1976) Oscillations of a Monsoon System. Part I. Observational Aspects. Journal of the Atmospheric Sciences 33:1937-1954

Lawrence DM, Webster PJ (2002) The Boreal Summer Intraseasonal Oscillation: Relationship between Northward and Eastward Movement of Convection. Journal of the Atmospheric Sciences 59:1593-1606

Lee J-Y, Wang B, Wheeler MC, Fu X, Waliser DE and Kang I-S (2012) Real-time multivariate indices for the boreal summer intraseasonal oscillation over the Asian summer monsoon region. Climate Dynamics 40:493-509

Lewis JM (1998) Clarifying the dynamics of the general circulation: Phillips's 1956 experiment Bulletin of the American Meteorological Society 79:39

Li RCY, Zhou W (2013) Modulation of Western North Pacific Tropical Cyclone Activity by the ISO. Part I: Genesis and Intensity Journal of Climate 26:2904-2918

Liebmann B, Smith CA (1996) Description of a Complete (Interpolated) Outgoing Longwave Radiation Dataset. Bulletin of the American Meteorological Society 77:1275-1277

Lindzen RS, Hou AV (1988) Hadley Circulations for Zonally Averaged Heating Centered off the Equator Journal of the Atmospheric Sciences 45:2416-2427

Liu Y, Hoskins B, Blackburn M (2007) Impact of Tibetan Orography and Heating on the Summer Flow over Asia Journal of the Meteorological Society of Japan Vol. 85B

Livezey RE, Chen WY (1983) Statistical Field Significance and its Determination by Monte Carlo Techniques. Monthly Weather Review 111:46-59

Lorenz EN (1967) The nature and theory of the general circulation of the atmosphere vol 218. World Meteorological Organization Geneva,

Lorenz EN (1983) A history of prevailing ideas about the general circulation of the atmosphere Bulletin of the American Meteorological Society 64:730-769

Madden RA, Julian PR (1972) Description of Global-Scale Circulation Cells in the Tropics with a 40–50 Day Period Journal of the Atmospheric Sciences 29:1109-1123

Masarik MT, Schubert WH (2013) Analytical solutions of the potential vorticity invertibility principle. Journal of Advances in Modeling Earth Systems 5:366-381

Matsuno T (1966) Quasi-geostrophic motions in the equatorial area J Meteor Soc Japan 44:25-43

McIntyre ME (2001) Balance, potential-vorticity inversion, Lighthill radiation, and the slow quasimanifold. In: IUTAM Symposium on Advances in Mathematical Modelling of Atmosphere and Ocean Dynamics, 2001. Springer, pp 45-68

McIntyre ME (2003a) Balanced flow Encyclopedia of Atmospheric Sciences 2:680-685

McIntyre ME (2003b) Potential vorticity Encyclopedia of Atmospheric Sciences 2:685-694

McIntyre ME (2008) Potential-vorticity inversion and the wave-turbulence jigsaw: some recent clarifications Adv Geosci 15:47-56

McIntyre ME, Norton WA (2000) Potential Vorticity Inversion on a Hemisphere. Journal of the Atmospheric Sciences 57:1214-1235

McIntyre ME, Palmer TN (1983) Breaking planetary waves in the stratosphere. Nature 305:593-600

Murakami T, Frydrych M (1974) On the Preferred Period of Upper Wind Fluctuations During the Summer Monsoon. Journal of the Atmospheric Sciences 31:1549-1555

Nielsen-Gammon JW (2012) Midlatitude synoptic meteorology: Dynamics, analysis, and forecasting. Wiley Online Library,

Ortega S, Webster PJ, Toma V, Chang H-R (2016a) Quasi-Biweekly Oscillations of the South Asian Monsoon: An observed link between the upper and lower level variability Submitted to Clim Dyn

Ortega S, Webster PJ, Toma V and Chang H-R (2016b) The Effect of Potential Vorticity Fluxes on the Tropical Upper Troposphere In preparation.

Persson AO (2006) Hadley's principle: understanding and misunderstanding the trade winds History of meteorology 3:17-42

Plumb RA, Hou AY (1992) The Response of a Zonally Symmetric Atmosphere to Subtropical Thermal Forcing: Threshold Behavior Journal of the Atmospheric Sciences 49:1790-1799

Popovic JM, Plumb RA (2001) Eddy Shedding from the Upper-Tropospheric Asian Monsoon Anticyclone. Journal of the Atmospheric Sciences 58:93-104

Postel GA, Hitchman MH (1999) A Climatology of Rossby Wave Breaking along the Subtropical Tropopause. Journal of the Atmospheric Sciences 56:359-373

Randel WJ, Park M (2006) Deep convective influence on the Asian summer monsoon anticyclone and associated tracer variability observed with Atmospheric Infrared Sounder (AIRS). Journal of Geophysical Research: Atmospheres 111

Rossby C-G (1936) Dynamics of steady ocean currents in the light of experimental fluid mechanics

Rossby, CG (1940) Planetary flow patterns in the atmosphere. Quarterly Journal of the Royal Meteorological Society 66 (Suppl.), 68—87

Sadler JC (1976) A Role of the Tropical Upper Tropospheric Trough in Early Season Typhoon Development. Monthly Weather Review 104:1266-1278

Saha K, Sanders F, Shukla J (1981) Westward Propagating Predecessors of Monsoon Depressions. Monthly Weather Review 109:330-343

Samelson R (2003) Rossby, Ertel, and potential vorticity

Schneider EK, Lindzen RS (1977) Axially symmetric steady-state models of the basic state for instability and climate studies. Part I. Linearized calculations Journal of the Atmospheric Sciences 34:263-279

Schubert W et al. (2004) English translations of twenty-one of Ertel's papers on geophysical fluid dynamics Meteorologische Zeitschrift 13:527-576

Schubert WH, Masarik MT (2006) Potential vorticity aspects of the MJO. Dynamics of Atmospheres and Oceans 42:127-151

Schwierz C, Dirren S, Davies HC (2004) Forced waves on a zonally aligned jet stream Journal of the atmospheric sciences 61:73-87

Scott R, Cammas J (2002) Wave breaking and mixing at the subtropical tropopause Journal of the atmospheric sciences 59:2347-2361

Scott R, Cammas J, Mascart P, Stolle C (2001) Stratospheric filamentation into the upper tropical troposphere J Geophys Res 106:835-811

Sikka DR (1977) Some aspects of the life history, structure and movement of monsoon depressions. Pure and Applied Geophysics 115:1501-1529

Sikka DR, Gadgil S (1980) On the Maximum Cloud Zone and the ITCZ over Indian, Longitudes during the Southwest Monsoon. Monthly Weather Review 108:1840-1853

Slingo JM (1998) Extratropical forcing of tropical convection in a northern winter simulation with the UGAMP GCM. Quarterly Journal of the Royal Meteorological Society 124:27-51

Tomas RA, Webster PJ (1994) Horizontal and Vertical Structure of Cross-Equatorial Wave Propagation. Journal of the Atmospheric Sciences 51:1417-1430

Vallis GK (2006) Atmospheric and Oceanic Fluid Dynamics. Cambridge University Press,

Waugh DW, Plumb RA (1994) Contour advection with surgery: A technique for investigating finescale structure in tracer transport Journal of the atmospheric sciences 51:530-540

Waugh DW, Polvani LM (2000) Climatology of intrusions into the tropical upper troposphere. Geophysical Research Letters 27:3857-3860

Weare BC, Nasstrom JS (1982) Examples of Extended Empirical Orthogonal Function Analyses. Monthly Weather Review 110:481-485

Webster PJ (1972) Response of the tropical atmosphere to local steady forcing Mon Wea Rev 100:518-541

Webster PJ (1973) Remote forcing of the time-independent tropical atmosphere Mon Wea Rev 101:58-68

Webster PJ, Chang H-R (1988) Equatorial energy accumulation and emanation regions: Impacts of a zonally varying basic state Journal of the atmospheric sciences 45:803-829

Webster PJ, Chang H-R (1998) Atmospheric wave propagation in heterogeneous flow: basic flow controls on tropical—extratropical interaction and equatorial wave modification Dynamics of Atmospheres and Oceans 27:91-134

Webster PJ, Holton JR (1982) Cross-Equatorial Response to Middle-Latitude Forcing in a Zonally Varying Basic State. Journal of the Atmospheric Sciences 39:722-733

Webster PJ, Hoyos CD (2004) Prediction of Monsoon Rainfall and River Discharge on 15-30-Day Time Scales. Bulletin of the American Meteorological Society 85:1745-1765

Webster PJ, Magaña VO, Palmer TN, Shukla J, Tomas RA, Yanai M and Yasunari T (1998) Monsoons: Processes, predictability, and the prospects for prediction. Journal of Geophysical Research 103:14451

Wu G, Duan A, Liu Y, Mao J, Ren R, Bao Q, He B, Liu B and Hu W (2015) Tibetan Plateau climate dynamics: recent research progress and outlook. National Science Review 2:100-116

Zhang C, Ling J (2011) Potential Vorticity of the Madden–Julian Oscillation Journal of the Atmospheric Sciences 69:65-78